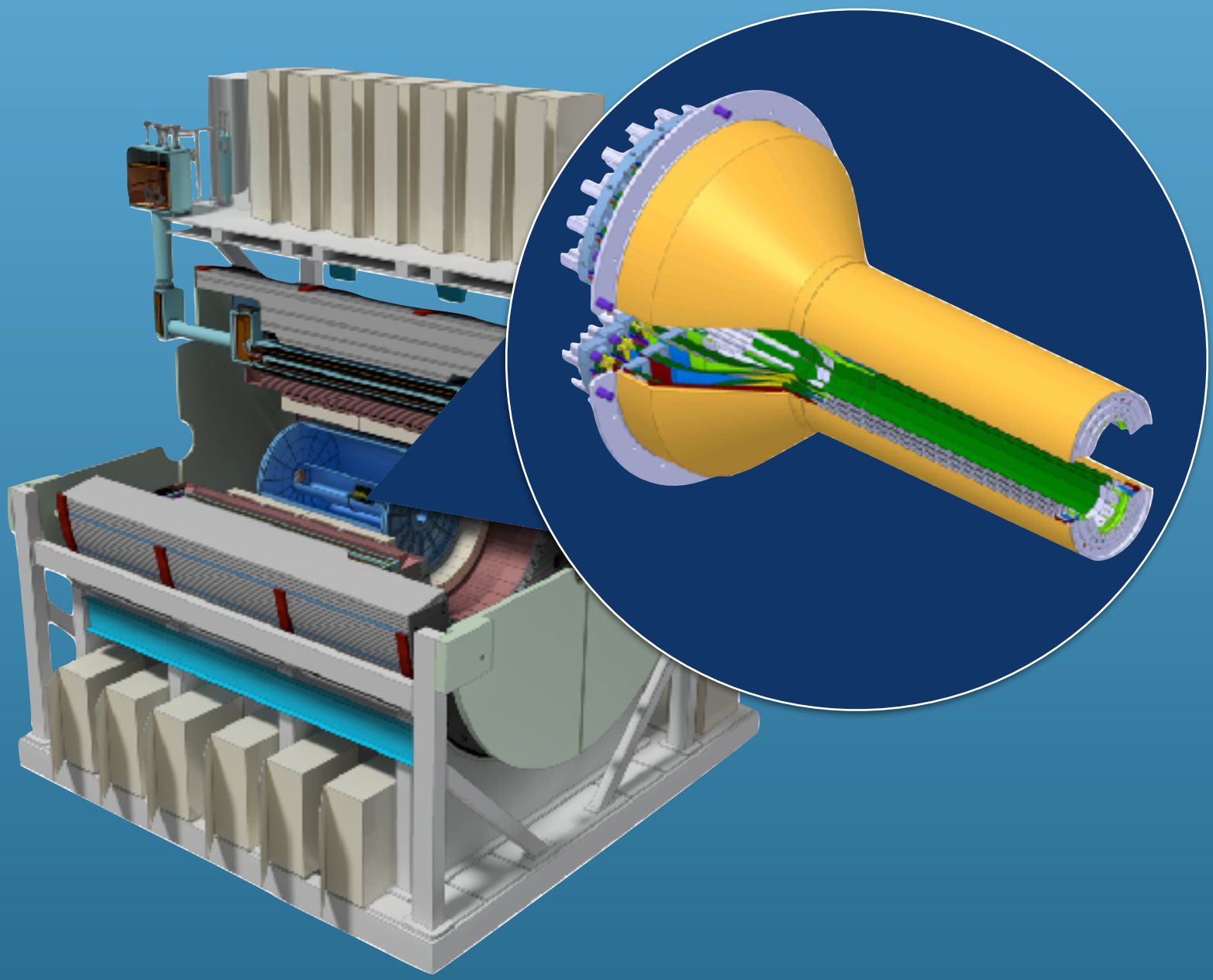

A Monolithic Active Pixel Sensor Detector for the sPHENIX Experiment

Monolithic-Active-Pixel-Sensor-based Vertex Detector (MVTX) proposal for the sPHENIX Experiment at RHIC

A proposal submitted to the DOE Office of Science
February 1, 2017

Invited Proposal:
DOE Office of Science Program Manager:

Proposing Organization:	Los Alamos National Laboratory
Collaborating Institutions:	Lawrence Berkeley National Laboratory Massachusetts Institute of Technology Brookhaven National Laboratory Univ. of California at Berkeley Univ. of California at Los Angeles Univ. of California at Riverside Central China Normal University Univ. of Colorado Florida State University Georgia State University Iowa State University New Mexico State University Univ. of New Mexico Univ. of Science and Technology of China Purdue University Univ. of Texas at Austin Yonsei University RIKEN/RBRC
Principal Investigator:	Ming X. Liu Phone: 505-412-7396 Email: mliu@lanl.gov
Requested Funding:	$4.9M, FY18-FY21

Table of Contents

Abstract

Title: Monolithic-Active-Pixel-Sensor-based Vertex Detector (MVTX) proposal for the sPHENIX Experiment at RHIC

Lead Institution: Los Alamos National Laboratory

Principal Investigator: Ming X. Liu

Co-Investigators: Grazyna Odyniec (LBNL) and Robert Redwine (MIT);

The goal of the sPHENIX experiment at the Relativistic Heavy Ion Collider (RHIC), which was granted DOE CD-0, is to study the novel properties of the quark-gluon-plasma that is believed to have existed a few microseconds after the Big Bang, when the entire universe was permeated with QGP at a temperature of several trillion degrees. Measurements at the Relativistic Heavy Ion Collider at Brookhaven National Laboratory (BNL) and the Large Hadron Collider (LHC) at CERN have both confirmed the existence of the QGP. The QGP created in collisions of heavy nuclei at very high energy has been seen to have novel emergent properties, such as very low viscosity close to the quantum limit. The ultimate goal for understanding the strong interaction under extreme conditions is to develop a microscopic description of this plasma, including the thermodynamic properties. Measurements of hadronic jets will reveal the internal structure of the QGP via their scattering with quasiparticles in the medium. Bottom quark jets (*b*-jets) and B-mesons produced in heavy ion collisions at RHIC offer a unique set of observables due to the large bottom quark mass, but need to be measured across an unexplored kinematic regime. These measurements of b-jets and B-mesons are essential to produce a complete understanding of the plasma. sPHENIX is a jet detector designed to collect a suite of unique jet observables with high statistics. Reconstruction and identification of b-jets and B-mesons requires both precision tracking of charged particles close to the beam collision point and high detection efficiency. We propose to build Monolithic-Active-Pixel-Sensor based precision vertex detector (MVTX) to ensure the sPHENIX inner tracker is capable of performing these key measurements.

1 Executive Summary

sPHENIX is a next-generation nuclear physics experiment providing world-class capabilities for multi-scale studies of the strongly coupled quark gluon plasma (QGP) planned for the Relativistic Heavy Ion collider (RHIC) at Brookhaven National Laboratory in 2022 and beyond. The need for these capabilities to advance our understanding of the origins of novel QGP properties is detailed in the 2015 NSAC Long Range Plan.

Precise measurements of heavy flavor-tagged jets and B-hadron nuclear modification and flow in heavy ion collisions are key scale-dependent observables. Measuring these rare observables demands high precison tracking with precise displaced secondary vertex capabilities. While the baseline sPHENIX detector anticipates a small aperture detector for secondary vertexing, exploiting the full potential of RHIC luminosity and optimizing the available running time is only possible with a large acceptance precision vertex detector. We propose to build a thin, extremely precise silicon pixel vertex detector for the sPHENIX experiment to enable these key measurements. The detector will be based closely on the latest generation of Monolithic-Active-Pixel-Sensor (MAPS) technology, developed for the ALICE collaboration at CERN, and leveraging the extensive R&D investments made in this technology over a period of several years. The sPHENIX MAPS Vertex Detector (MVTX) is proposed to be ready for Day-1 sPHENIX data taking.

The detector described in this proposal will provide world-class scientific results in key areas encompassed by the DOE Nuclear Physics mission. It will allow U.S. scientists to explore fundamental questions into the nature of the QGP that cannot be probed with other existing facilities worldwide. In particular, the sPHENIX experiment, which was granted with DOE CD-0 in September 2016, will complement and extend the ongoing and future QGP studies at RHIC and LHC, and will become the next generation U.S. flagship high energy nuclear physics program at the DOE's key facility in this field.

2 Physics Goals

The physics goals of the proposed vertex detector project are aligned with the key challenges and physics opportunities outlined in the 2015 NSAC Long-Range Plan: "There are two central goals of measurements planned at RHIC, as it completes its scientific mission, and at the LHC: (1) Probe the inner workings of QGP by resolving its properties at shorter and shorter length scales. The complementarity of the two facilities is essential to this goal, as is a state-of-the-art jet detector at RHIC, called sPHENIX. (2) Map the phase diagram of QCD with experiments planned at RHIC."

The key approach for goal (1) is microscopy of the QGP through probes that are sensitive to characteristic scales in the plasma. The baseline sPHENIX design is optimized to employ light quark and gluon jets over a wide kinematic range and Upsilons as such scale-sensitive probes. The vertex detector described in this proposal will greatly expand the sPHENIX capabilities in an additional dimension related to scales in the QGP, by allowing a range of precision studies as a function of parton mass. Studies of heavy-flavor hadrons have been a focus of recent upgrades in PHENIX and STAR at RHIC. These studies, as well as new measurements by the current LHC experiments form the key motivation for the ALICE Phase-I upgrades for the early 2020's. In combination with the large acceptance and high rate capability of sPHENIX, the vertex detector upgrade provides access to observables that are not accessible with the present RHIC detectors and are complementary to those at LHC.

Heavy flavor quarks (c, b) play a unique role for studying the QCD in vacuum as well as at finite temperature or density. Their masses are much larger than the QCD scale ($\Lambda_{\rm QCD}$), the additional QCD masses due to chiral symmetry breaking as well as the typical medium temperature created at RHIC and

LHC. Therefore they are created predominantly from initial hard scatterings and their production rates are calculable in perturbative QCD. Thus they are calibrated probes that can be used to study the QGP in a controlled manner.

The vertex detector will enable a wide range of heavy-flavor studies, such as extending present RHIC measurements to significantly larger transverse momenta. A particular new capability, in combination with the sPHENIX calorimetric jet reconstruction, is the identification of jets originating from heavy quarks. In this proposal, we will use the measurements of b-tagged jets as a case study to illustrate the new capabilities the upgrade brings to RHIC and the overall field. This particular measurement represents both a new opportunity at RHIC and an example of complementary to the LHC: the projected sPHENIX measurement both extends the LHC measurement to lower transverse momenta and provides a kinematic overlap, where the same jets can be studied in the different QGP conditions at RHIC and LHC.

2.1 B-meson physics at low p_{T}

As revealed by the single-electron nuclear modification factor R_{AA} data at RHIC, heavy quarks lose energy when traversing the QGP medium through both radiative mechanism as well as elastic collisional mechanism [1, 2]. Recent Charm-hadron data from RHIC and LHC show their R_{AA} are quite similar to those of light flavor hadrons [3, 4]. Theoretical calculations predict that Bottom-hadrons should be much less suppressed compared to charm and light flavor hadrons due to the much larger bottom quark mass in the p_{T} region of 5-20 GeV/c at RHIC [5]. To systematically understand the flavor/mass dependence of parton energy loss mechanism, the next physics goal would be to measure and understand the bottom hadron production in heavy ion collisions.

Another unique feature that heavy quarks bring is that their motion inside the QGP medium can be treated in analogy to the Brownian motion when their masses are much larger than every momentum kick they suffer in the QGP. Therefore, one can simplify their dynamics through the QGP with a Langevin simulation and then access the heavy quark spatial diffusion coefficient ($2\pi TD_s$), the QGP medium transport parameter by comparing data and model calculations. Recent STAR HFT measurements reveal that the Charm-hardon v_2 follows the same empirical ($m_{\mathrm{T}} - m_0$) scaling as light hadrons at $p_{\mathrm{T}} < 4$ GeV/c [6]. This suggests charm quarks may have reached the thermal equilibrium. On the other hand, theoretical calculation also shows the Langevin simulation for charm quarks may have sizable corrections compared to the full Boltzmann transport [7]. To precisely determine the intrinsic QGP transport parameter, D_s, measurements of bottom hadron production, particularly at low p_{T}, will be critical.

Furthermore, measuring the total bottom cross section in heavy ion collisions will be also crucial for the interpretation of the suppression in the bottomonia production, which is one of the highlighted sPHENIX measurements that has been proposed. In addition, a time of flight (TOF) detector with the timing resolution of 40ps or less is under discussion in sPHENIX. Particle identification capability will be greatly enhanced should the TOF realized and so will be the the overall physics program at sPHENIX.

2.2 b-jet physics at intermediate p_{T}

Measurements of jets provide more information on the initial parton kinematics and how it is affected by the QGP medium. Given their large energy compared to single hadrons, jets probe a smaller spatial scale of the medium, revealing its microscopic structure and possibly a different magnitude of coupling with the medium. Jets containing b-quarks are particularly interesting because of the large quark mass. Bottom quarks, which are $\sim$1000 times heavier than the light quarks, produce unique energy loss signatures due to their large mass (4.2 GeV/c^2). At momenta comparable to this scale, bottom quarks will preferentially lose energy via collisions with the plasma quasi-particles and not via gluon radiation, which is predominant for light quarks.

Jets containing b-quarks are also distinct from light-quark jets in their high multiplicity and hard fragmentation, where the leading particle typically carries 70-80% of the jet energy. Measurements of b-jets in Pb+Pb collisions at LHC cover momenta larger than 80 GeV/c. Surprisingly, these measurements indicate a nuclear modification factor very similar to inclusive jets [8]. One of the explanations is that the mass of the quark is irrelevant for a 80 GeV/c jet. The other hypothesis is that given that most of b-jets at LHC are from gluon splitting processes, the jet containing a b-quark still behaves as a massive color octet object when crossing the medium, resembling a massive gluon [9]. None of these disadvantages are present at RHIC energies since

1. b-jets can be measured with momentum as low as 15 GeV/c, where the quark mass is more important for the energy loss mechanisms

2. the main process producing b-jets at RHIC is the leading order gluon fusion ($g + g \rightarrow b + \bar{b}$) and excitation of intrinsic b-quarks in the proton wave function ($b + g \rightarrow b + g$). The b-quark produced in these processes crosses the medium as massive quark (color triplet state).

3 Detector Requirements

3.1 The sPHENIX detector capability

The planned sPHENIX detector [10, 11] is designed to perform measurements of jets, quarkonia in p+p and heavy ion collisions at RHIC. The baseline sPHENIX detector consists of a tracking system and a calorimeter system, both of which which have full 2π acceptance in azimuth and a pseudorapidity coverage of $|\eta| < 1$ and is assembled around a 1.4 Tesla superconducting magnet coil. The sPHENIX calorimeter system includes an electromagnetic calorimeter and an inner hadronic calorimeter, which sit inside a solenoid coil, and an outer hadronic calorimeter located outside of the coil. The baseline tracking system includes a strip intermediate silicon tracker (INTT) and a outer time projection chamber (TPC) and allows addition of an inner vertex tracker.

The sPHENIX baseline detector packages allows calorimetry based triggering and measurement of jets at RHIC with an energy resolution of $\Delta E/E = 120\%/\sqrt{E}$ and contains 80% of opposite di-jet pairs from the same hard-collision. The electromagnetic calorimeter provides trigger, identification and measurement of high-energy electrons with an energy resolution better than $\Delta E/E = 15\%/\sqrt{E}$. The tracking momentum resolution is 1-2% in the transverse momentum range of 0-10 GeV$/c$, which allows reconstructing Upsilon invariant mass resolution of around 80 MeV. The DAQ system is designed to provide calorimetry-based trigger on jets and Upsilon signals, and to record full detector events at 15 kHz, which matches the collision rate delivered by RHIC within a vertex range of $|z| < 10$ cm.

3.2 Physics driven detector requirements for MVTX

In order to deliver the desired physics goals, requirements are placed on the detector design in the following aspects:

- **Acceptance**: both b-jet and B-meson physics programs are statistically limited. Therefore, the inner tracking detector should match the acceptance for the planned sPHENIX detector in order to provide precision vertex displacement measurement for all tracks detected by sPHENIX. The detector should have full coverage of $|\eta| < 1$ for charged tracks with hits in at least two MVTX layers for events within $|z| < 10$ cm.

- **Event rate**: the b-jet physics program requires sampling a large number of events with inclusive jets and the B-meson physics program requires high statistics minimum biased Au+Au collision events. Since both programs are statistically limited, the inner tracker should deliver an event rate not lower than the sPHENIX trigger rate of 15 kHz.

- **DCA resolution**: The $c\tau$ for D and B decays is about 120 μm and 460 μm, respectively, and the Distance of Closest Approach (DCA) with respect to the primary vertex of these heavy-flavor mesons is larger than prompt particles. Therefore it is crucial to have a good DCA resolution (< 50 μm at $p_T > 1$ GeV/c) to distinguish tracks from heavy flavor hadron decay. In order to achieve the required DCA resolution down to $p_T > 1$ GeV/c, where multiple scattering is dominating, it is very important to reduce the material budget of inner tracking detector.

- **Efficiency**: The b-jet physics program requires simultaneous detection of a few displacement tracks from B-meson decay within the jet; the B-meson physics program requires detection of both of the decay particle tracks from the $B \to D \to \pi^{\pm}K^{\mp}$ decay chain. Therefore, good tracking efficiency is required, i.e. a minimal efficiency 60% at p_T =1 GeV/c in central Au+Au collisions in order to deliver the minimal purity and efficiency for b-jet tagging.

These requirements are summarized in Table 1.

Item	Requirement
Acceptance	Vertex $\lvert z\rvert$ <10 cm, $\lvert\eta\rvert < 1$, full azimuthal coverage
Event rate	Matching the sPHENIX DAQ rate of 15 kHz event rate
DCA resolution	< 50 μm for charged pions at p_T =1 GeV/c
Tracking efficiency	$> 60\%$ efficiency for charged pions at p_T =1 GeV/c in central Au+Au collisions

Table 1: Summary for the vertex detector requirements

4 Technology Choices and Detector Layout

We propose to adopt the ALICE Inner Tracking System (ITS) Upgrade 3-layer MAPS-based Inner Barrel (IB) detector design, with minimal modifications to both electrical and mechanical systems, for use in the sPHENIX experiment. A full description of the ITS Upgrade can be found in the Technical Design Report [12].

Figure 1 shows the side view of ALICE ITS IB mounted on the sPHENIX beam pipe. Sitting outside of the MVTX is the intermediate silicon strip tracker (INTT) planned to be funded by the RIKEN research institute in Japan. With single-event response and spatial resolution between that of the MVTX detector and that of the TPC, the INTT is intended to help pattern recognition in heavy ion and p+p collisions. The precise geometry and configuration of the INTT is being optimized, and that effort is not part of this proposal.

4.1 Design goals and technology choice

Recent developments in the technology of Monolithic-Active-Pixel-Sensors (MAPS) have made it possible to have sensor designs with high speed, fine granularity, minimal radiation length and low power at relatively low cost. The ALPIDE sensor [13, 14] developed for the ALICE ITS Upgrade has attributes that meet the sPHENIX requirements. We have focused our design on leveraging the extensive R&D work already done for the ALICE ITS. We intend to use the ALICE ITS design of the inner three layers of the

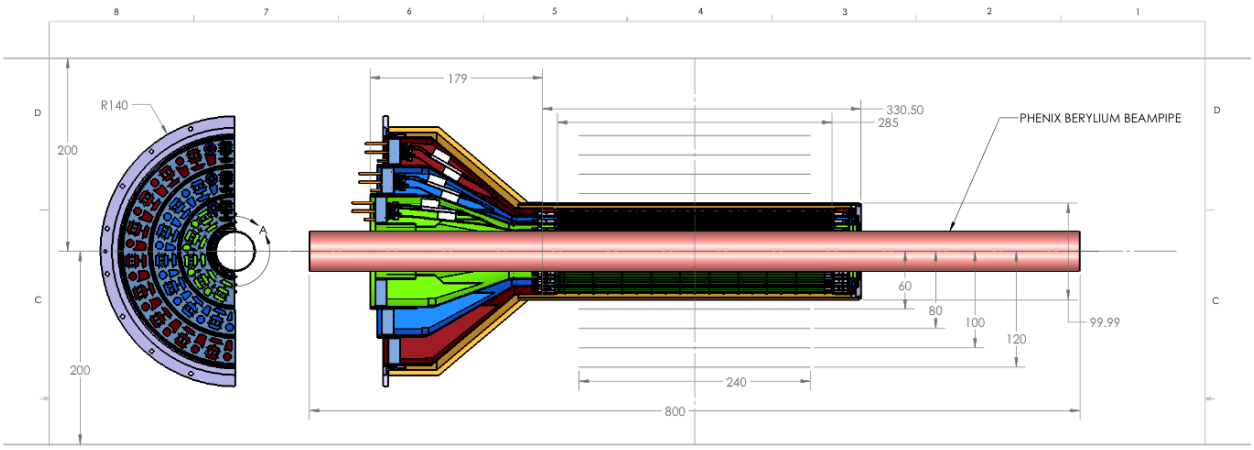

Figure 1: Side view of MVTX, showing its location relative to the sPHENIX beam pipe.

ALICE ITS as the primary baseline design for the sPHENIX inner tracking detector. This will be the basis of the designs and plans of the proposed sPHENIX MVTX detector. On the basis of the requirements considerations of Section 3, the proposed solution for the layout of the sPHENIX vertex detector is a 3-layer silicon barrel based on the technology of Monolithic Active Pixel Sensors. To meet the required capabilities in terms of displaced vertex resolution, tracking efficiency and readout rate, the requirements for the sPHENIX vertex detector are summarized here:

- The track pointing resolution is mainly determined by the two innermost measurements of the track position. This requires the first detection layer be as close to the beam line as possible. Three layers provide redundancy against failure of detector modules. The radial distance between the three layers as small as possible, to preserve the two innermost measurements of the track position if one of the points close to the primary vertex is not attached to it.

- Reduction of material budget to minimize multiple-scattering track distortion. Reducing the material budget of the first detection layer is particularly important for improving the impact parameter resolution.

- The segmentation of the detector determines the intrinsic spatial resolution of the reconstructed track points. Excellent spatial resolution of the first layer is key for the resolution of the impact parameter at high particle momentum where the effect of the multiple scattering becomes negligible. Fine segmentation is also important to keep the occupancy low.

- Short integration time window to minimize the event pile-up and keep the occupancy at a low value when reading out the detector at the expected rate of 15 kHz.

These design goals lead to a vertex detector configuration consisting of three concentric layers of pixel detectors. Monolithic Active Pixel Sensors implemented using the 0.18 μm CMOS TowerJazz technology and developed by the ALICE collaboration at CERN are an ideal technology for the three layers. The basic active MVTX element is the Pixel Chip. It consists of a single silicon die of about 15 mm x 30 mm, which incorporates a high-resistivity silicon epitaxial layer (sensor active volume), a matrix of charge collection diodes (pixels) with a pitch of about 30 μm, and the electronics that perform signal amplification, digitization and zero-suppression. Only the information on whether or not a particle crossed a pixel is read out. The

main functional elements of the sPHENIX MVTX detector are introduced in the following section, while its main geometrical parameters are listed in Table 2.

	Layer 0	Layer 1	Layer 2
Radial position (min.) (mm)	22.4	30.1	37.8
Radial position (max.) (mm)	26.7	34.6	42.1
Length (sensitive area) (mm)	271	271	271
Active area (cm^2)	421	562	702
Number of pixel chips	108	144	180
Number of staves	12	16	20

Table 2: Parameters of the sPHENIX MVTX design.

4.2 Detector layout

The proposed sPHENIX MVTX detector is designed to leverage the extensive research and development behind the design of the ALICE ITS Upgrade Inner Barrel. In the ALICE design, the layers are azimuthally segmented in units called staves, which are mechanically independent. Staves are fixed to a support structure, half-wheel shaped, to form half-layers. The stave and the half-layer are shown in Figure 2).

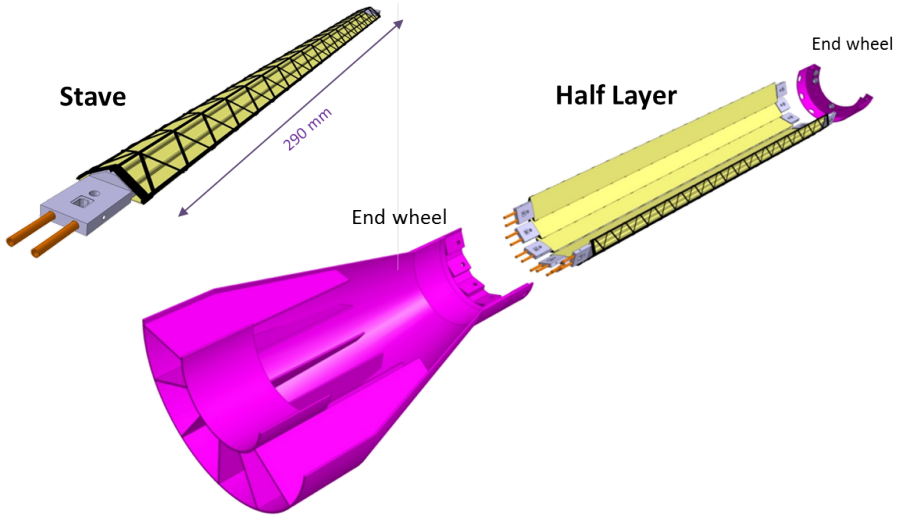

Figure 2: MVTX Stave and Half-Layer: each half-layer is composed of a set of staves fixed to wheel-shaped support structures. The layout shown here is based on the ALICE ITS Upgrade Inner Barrel design.

The term Stave will be used to refer to the complete detector element. It consists of the following main components:

- Space Frame: a truss-like lightweight mechanical support structure for the single stave based on composite material (carbon fiber).
- Cold Plate: carbon ply that embeds the cooling pipes.
- Hybrid Integrated Circuit (HIC): assembly consisting of the polyimide flexible printed circuit (FPC) on which nine Pixel Chips and some passive components are bonded.

Each Stave will be instrumented with one HIC, which consists of a row of nine Pixel Chips glued and connected to the FPC, hence covering a total active area of 15 mm x 271.2 mm including the 150 μm gap between adjacent chips along z. The interconnection between Pixel Chips and FPC is achieved via wire bonding. The HIC is glued to the Cold Plate with the Pixel Chips facing it in order to maximize cooling efficiency. An extension of the FPC connects the Stave to a patch panel that is served by the electrical services entering the detector from one side only. A mechanical connector at each end of the Stave allows the fixation and alignment of the Stave itself on the end-wheels, as described in Section 6.3. The inlet and outlet of the closed-loop cooling circuitry are located at the same end of the Stave because the cooling is also served from the same side as all other services. The prototyping of the Stave is well advanced. The design of the Stave accounts for the tight requirement on the material budget, which is limited to 0.3% X_0.

The three layers are then integrated together and with an outer cylindrical structural shell (CYSS) to form two detector halves, as shown in Figure 3).

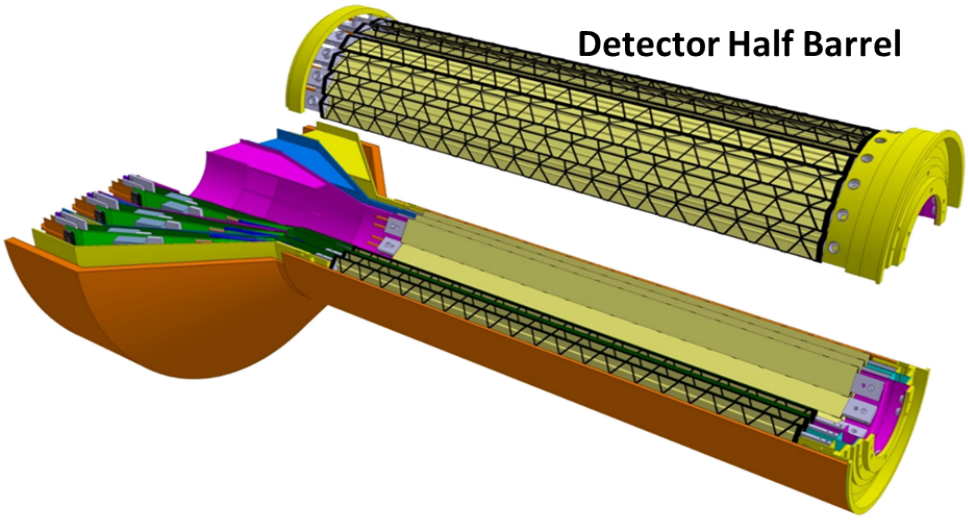

Figure 3: MVTX 3-layer Detector Barrel: each half-barrel is composed of a detector section and a services section. The layout shown here is based on the ALICE ITS Upgrade Inner Barrel design.

5 Physics Performance

We discuss the expected tracking performance of the MVTX in the sPHENIX experiment. MVTX is the key device in sPHENIX to provide the precision measurement of the primary vertex as well as the displaced secondary tracks from heavy quark decays. Figure 4 shows the single track efficiency and the DCA pointing resolution in the bending plane as a function of p_T based on the full GEANT4 detector simulation plus the offline tracking software reconstruction (see Section 6.9 for offline simulation and tracking). The efficiencies were evaluated using charged pion tracks embedded in central (i.e., high multiplicity) HIJING events. The single track efficiency is about 80% at 1 GeV/c and the DCA pointing resolution is about 40 μm for 0.5–1 GeV/c tracks. These performance parameters meet detector requirements based on the full detector simulation study.

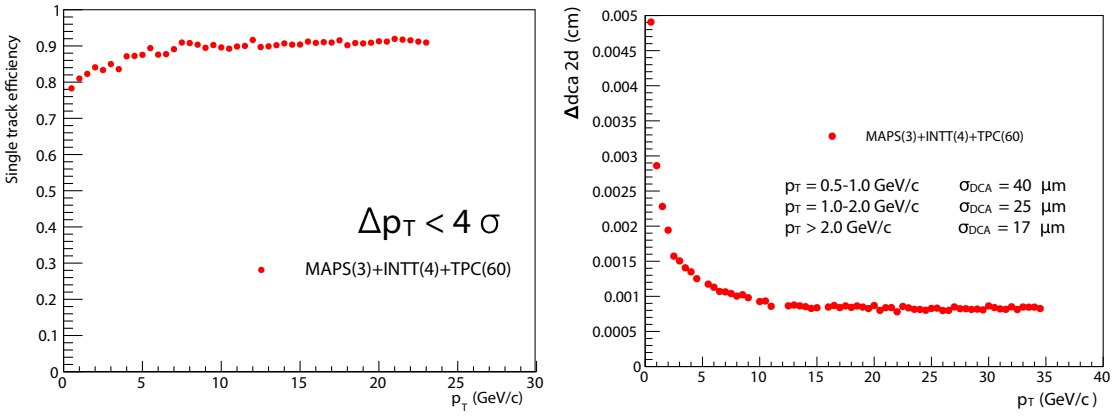

Figure 4: Single track reconstruction efficiency (left) and DCA pointing resolution in the bending plane (right) in central Au+Au collisions from full HIJING plus GEANT4 simulation.

5.1 *b*-jet tagging

Detection of *b*-jets with the sPHENIX detector is complicated by the comparative rarity of *b*-jets, as shown in the left panel of Figure 5, and also by the significant background of the underlying event in heavy ion collisions. Multiple exploratory methods have been developed and demonstrate the the proposed MAPS detector enables *b*-jet tagging in sPHENIX, and enable cross check of the systematic uncertainties. As shown in the right diagram of Figure 6, these methods are based on the unique features of *B*-hadron decays, including finite decay length and leptonic decay products. These methods are:

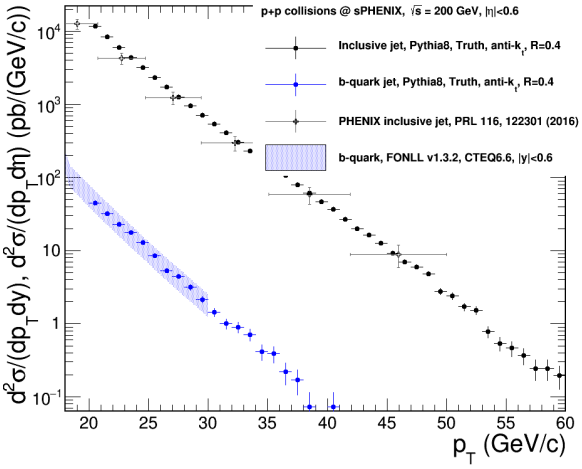

Figure 5: Comparison of the cross section for b-jets (blue) and all jets (black). *b*-jets are rare compared to the much more abundant light quark jets.

- Identify *b*-jets by requiring multiple tracks within the jet cone that do not originate from the primary collision vertex. These are likely be the long-lived *B*-hadron decay products. As an initial study, we performed full sPHENIX detector simulation to demonstrate such capability in $p+p$ collisions as shown in the left panel of Figure 7 and 8. Despite the simplified algorithm used in this exploration,

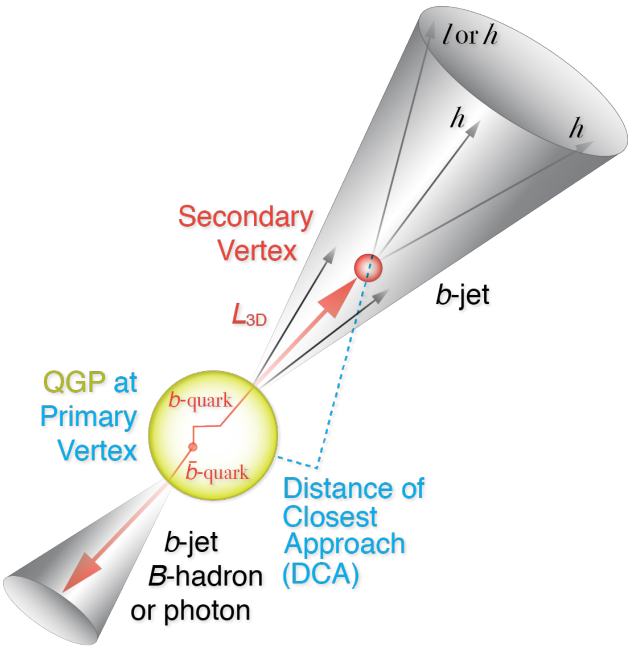

Figure 6: A b-quark traverses the QGP and fragments into a b-jet. The principles of tagging the rare b-jets are based on unique features of B-hadrons: long life time and finite decay length of B-hadron ($L3D$ ~few mm), decay tracks from secondary vertices and leptonic decay products.

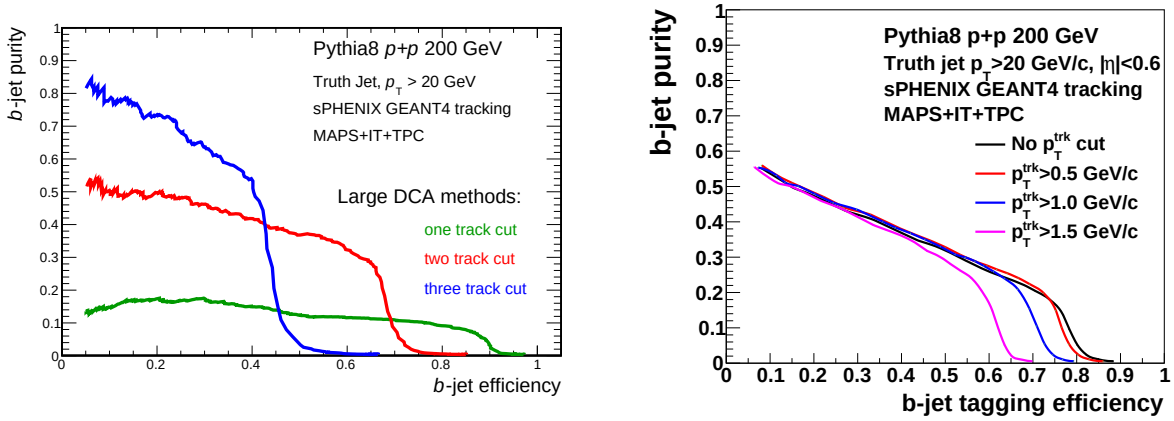

Figure 7: Projected b-jet tagging performance study in p+p collisions.

the b-tagging performance approaches that seen by CMS in their b-jet analysis at much higher energy [8, 15]. Before the data taking of the MVTX project, many techniques will be developed in the final software to achieve the best performance, including likelihood analysis, 3-dimensional track displacement and machine learning techniques.

- Identify b-jets by requiring multiple tracks within the jet cone to come from the same displaced secondary vertex distinct from the primary vertex. This method is related to the previous one; however it also uses the knowledge that a B-hadron is likely to decay into multiple daughter particles. This provides additional power in selecting and cross checking b-jet candidates identified via the first method.

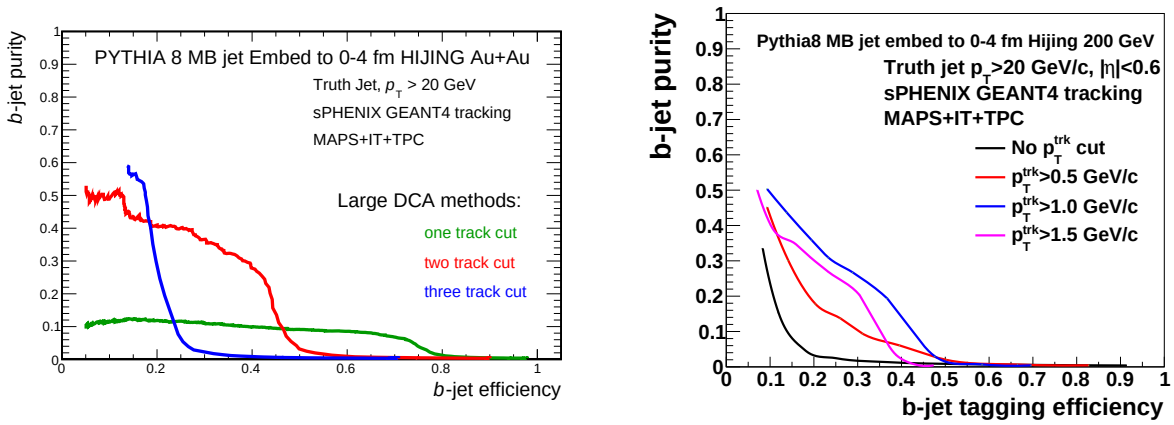

Figure 8: Preliminary projection of b-jet tagging performance study in Au+Au collisions. The tracking software is not yet fully optimized, however the performance curves allow an analysis working point of 30-40% purity at 30-40% b-jet efficiency as used in the existing analysis performed at LHC energy [8].

We also demonstrated this method in full simulation as shown in the right panel of Figure 7 and 8. This method also provide data driven quantification of b-jet purity via secondary vertex kinematics fitting.

- Identify b-jets by requiring electron or positron tracks to be detected within the originally identified jet cones. Utilizing the fact that B-hadrons have a significant chance (20%) to decay to a leptonic final state, this is a nearly orthogonal method that could provide an independent cross check of both methods above. We will explore its feasibility in the sPHENIX environment and performance projections for such cross checks.

After the initial identification of b-jet candidates, the purity of b-jets in the candidate sample will be quantified in a data-driven way using the invariant mass and transverse momentum of the secondary vertex, which has proven to be critically important in the LHC environment [8, 15]. The projected uncertainty of the nuclear modification of inclusive b-jet is shown in Figure 9, which places stringent tests on the models describing the coupling between heavy quarks and the QGP [9]. We are in close collaboration with theory groups to update the model predictions of inclusive b-jet nuclear modification at the RHIC energy in the sPHENIX kinematic region.

Beyond the inclusive b-jet nuclear modification measurement, additional techniques in jet substructure and correlation studies will be enabled by the MVTX detector. Inclusive b-jets can originate from a high-energy b-quark (a true b-quark jet) or from a gluon that splits into b-quark and b-antiquark ($g \rightarrow b\bar{b}$-jet). These two categories of b-jets could potentially have very different interactions with the QGP, because in the latter case the correlated b-quark and b-antiquark traverse coherently through the QGP in a color octet state with two times of b-quark mass [9]. Although inclusive b-jets are expected to be dominated by the b-quark jets [16], the remaining $g \rightarrow b\bar{b}$-jet component could complicate the interpretation the inclusive b-jet results. MVTX detector will allow us to discriminate these two categories of b-jet productions and provide cleaner access to the dynamics of high energy b-quark interactions with the QGP:

- Correlation studies for b-jets: the fraction of true b-quark jets can also be enhanced by selecting b-quark partonic production channels. This is achieved by requiring the b-jet candidate be correlated

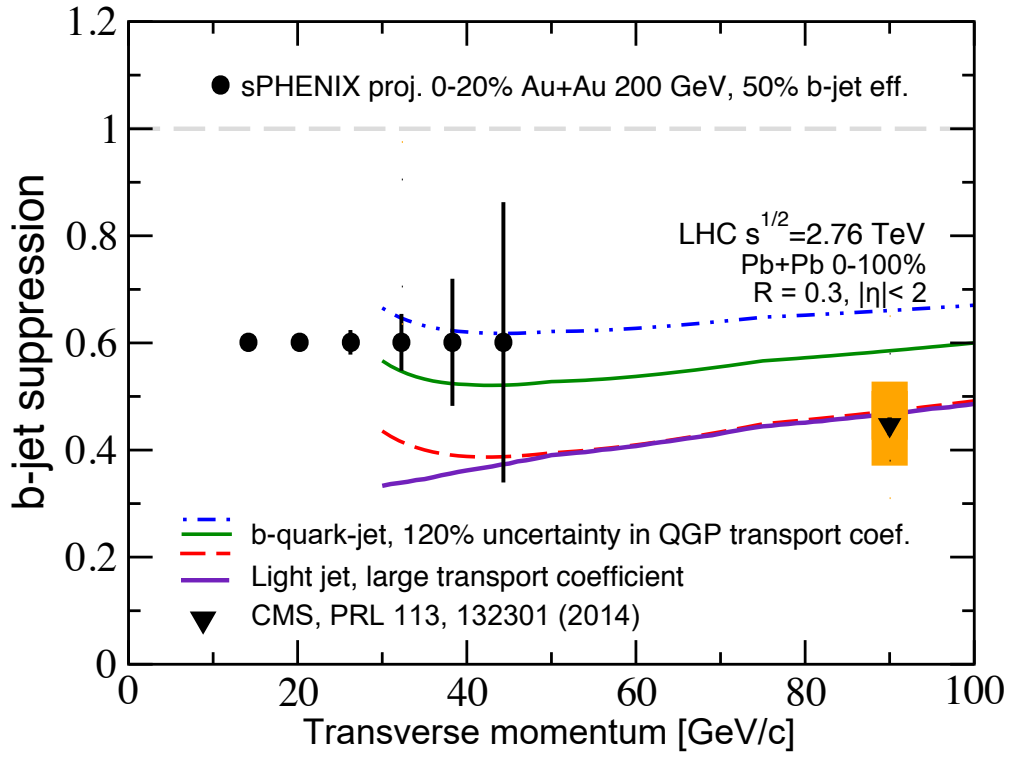

Figure 9: Projection of sPHENIX inclusive b-jet data in terms of the nuclear suppression factor (black circles), which is compared with CMS data (black triangles) [8], and QGP transport models for b-quark jets evaluated at the LHC energy (curves) [9]. sPHENIX with the proposed MAPS vertex detector will bring new data to RHIC energy and to the 15-40 GeV$/c$ transverse momentum region in which b-quarks move slowly and are predicted to show strong deviations from light quark jets. The inclusive b-jets at RHIC energy are expected to be dominated by b-quark jets [16]. The proposed b-jet substructure and correlation studies will also enhance the selection of b-quark jets (See text for details).

with another b-jet, B-hadron, or photon in the same event [17], as illustrated in Figure 6. In particular, correlations between two b-jets can be measured with high statistics using MVTX and sPHENIX detectors, taking advantage of their high rate capability and their large instrumented acceptance (covering nearly 80% of produced di-jets). A preliminary projection of transverse momentum balance of b-jet pairs is shown in Figure. 10, which is comparable precision with a recent results from Pb+Pb collision at $\sqrt{s_{NN}} = 7$ TeV measured by the CMS collaboration [15].

- Jet substructures: in recent years, the field of high-energy physics has developed a set of techniques to inspect the substructure of jets, to tag boosted objects and to differentiate between gluon and quark jets. These techniques have recently been adopted to study the interplay between light-jet probes with the QGP medium at the LHC [18] and at RHIC [19]. These techniques can also be utilized in identifying true b-quark jets for sPHENIX. Specifically, so-called jet grooming algorithms will be used to remove soft radiation from the jet, and to identify two leading subjet structures that correspond to the earliest splitting of the initiating parton [20]. In the leading order picture, the transverse momentum of the two subjets is likely be similar in a $g \to b\bar{b}$-jet, and in true b-quark jets, one subjet would likely dominate. Therefore, a measurement of transverse momentum ratio of the two subjets will be used to identify and quantify the purity of the true b-quark jets. A secondary vertex that is found by the MAPS detector that associates with the subjets can further confirm the b-quark origin of the subjets.

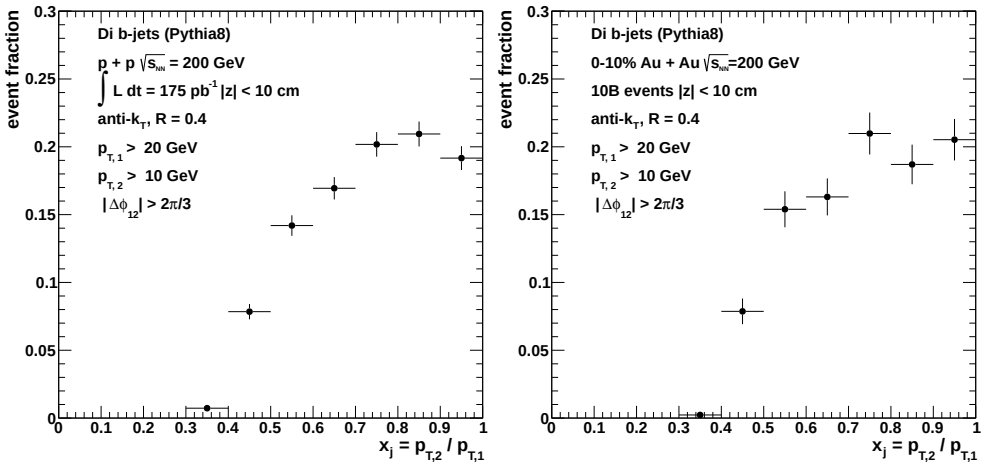

Figure 10: Preliminary projection of transverse momentum balance of b-jet pairs as enabled by the MVTX detector, for p+p (left) and for 0-10% central Au+Au collisions at $\sqrt{s_{NN}} = 200$ GeV.

5.2 B-meson tagging

The B-meson production can be studied through either inclusive decay daughters, e.g. D-mesons, J/ψ or $e^{\pm}$ via the impact parameter method or exclusive reconstruction, e.g. $D+\pi$ or $J/\psi+K$ etc via the secondary vertex reconstruction. These channels offer the sensitivity to access the low-p_T B-mesons. The fast MAPS silicon detector can efficiently separate the B-meson decay signals from the background dominantly coming from the primary interaction vertex in heavy-ion collisions.

One major challenge for separating low-p_T B-meson decays from the primary vertex is the background tracks that coming from the primary heavy-ion collisions. In the following, we will show the B-meson signal significance through the non-prompt D^0 channel using the full GEANT4/tracking simulation + a fast Monte Carlo method. The GEANT4/tracking simulation offers the tracking efficiency together with the MAPS detector plus the full DCA distributions of the charge tracks pointing to the primary vertex. These are fed into a fast Monte Carlo simulation that can be conducted with sufficient statistics for both signal and background evaluations.

Figure 11 left plot shows the D^0 DCA distributions to the primary vertex in the p_T of 4-5 GeV/c for 100M 0-10% central Au+Au events.. The narrow peak close to zero indicates the prompt D^0 signal from the primary collisions. The red distribution presents the signals from B-meson decays. The estimated background contribution is also shown in the same plot as the blue histograms.

Figure 11 right plot shows the estimated prompt and non-prompt D^0 significance as a function of p_T for 10 billion 0-10% central Au+Au collisions at $\sqrt{s_{NN}} = 200$ GeV taken with the sPHENIX and MVTX detectors. The red squares are estimated non-prompt D^0 significance with an additional Time-Of-Flight (TOF) detector for particle identification (assuming clean PID up to 1.6 GeV/c for kaons). The prompt D^0 production rate is taken from existing STAR measurements[6] and the B-meson production rate is based on the FONLL pQCD calculation in $p+p$ collisions and scaled with number-of-binary collisions to central Au+Au collisions. The estimation shows good performance for B-meson tagging using the non-prompt D^0 in a wide p_T region. The additional TOF detector would enhance the non-prompt D^0 measurement especially in the low p_T region.

We take the above significance estimation and convert to the statistical uncertainties on the physics observables - nuclear modification factor R_{CP} and v_2 for 100 billion Au+Au 200 GeV events, shown in Fig. 12. The left figure clearly shows that one can separate the non-prompt D^0 R_{CP} from the prompt D^0

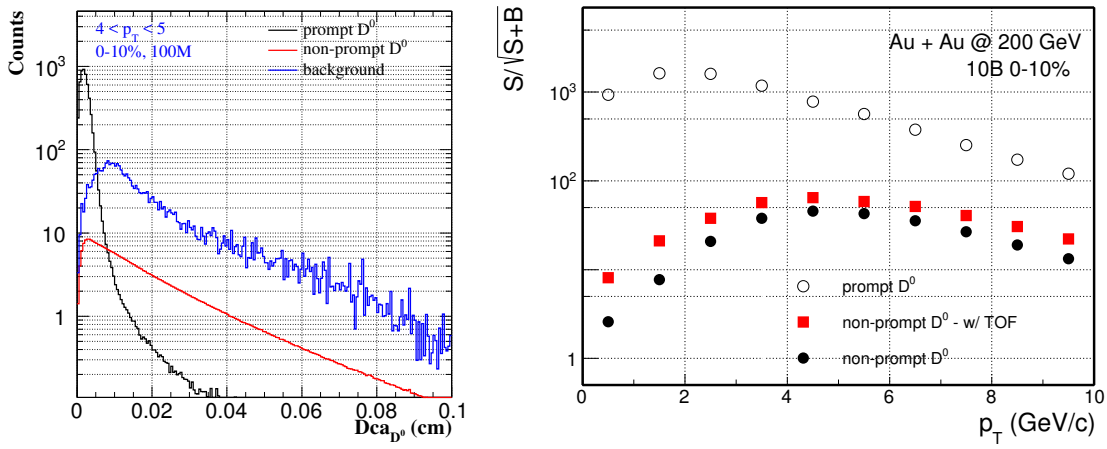

Figure 11: (Left) Simulated D^0 DCA distributions for prompt (black), non-prompt (red) as well as background (blue) contributions for 100M 0-10% central Au+Au events. (Right) Estimated prompt and non-prompt D^0 significance as a function of p_T for 10 billion 0-10% central Au+Au collisions at $\sqrt{s_{NN}} = 200$ GeV with sPHENIX MVTX detector. The red squares represent the estimated significance for non-prompt D^0 with a TOF detector for particle identification.

provided the suppression hierarchy predicted by theory calculations [5, 21, 22] holds. In the right figure, the estimated uncertainty shows that one can clearly answer the question whether bottom quarks flow with the medium or not. Such a precision should allow further joint efforts between theorists to further constrain the heavy quark diffusion coefficient, the intrinsic transport parameter of the sQGP.

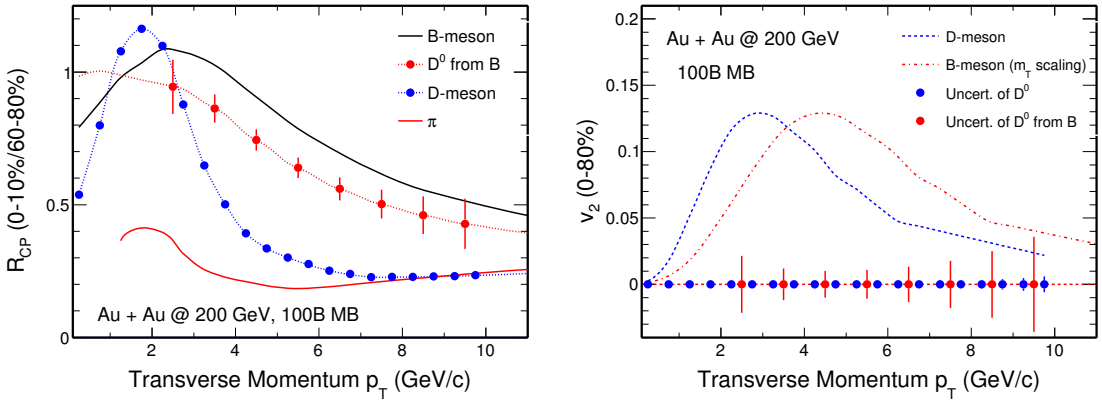

Figure 12: Statistical uncertainty estimation for R_{CP} (left) and v_2 (right) of non-prompt D^0 measurements from 100 billion Au+Au 200 GeV events. In the left plot, the D-meson and B-meson curves are based on calculations from Duke, TAMU and CUJET groups for 0-10% R_{AA} [5, 21, 22], and the dashed curve represents the non-prompt D^0 from B-meson decays. In the right plot, the D-meson curve is a fit to STAR recent D^0 v_2 data points [6] and the B-meson curve is calculated from the D-meson assuming the m_T scaling. The blue and red data points with the vertical bars indicate the statistical uncertainty projections for both D-meson and non-prompt D^0 (B decays) measurements.

The performance described above has been focused on the inclusive non-prompt D^0 channel. Simulations have been pursued to continue exploring the B-meson tagging using non-prompt J/ψ's or further exclusive reconstruction of B-meson through hadronic decays.

5.3 Event pileup effects

With the projected high RHIC beam luminosity, collision rate up to 2 MHz (100 kHz) is expected for p+p (Au+Au) collisions in sPHENIX. Since the integration time of MVTX MAPS chip is about 2 μs (37 beam crossings), a pile-up of hits from multiple collisions during this signal integration time window is expected for triggered events. Based on these numbers, on average, 8 (0.4) pile-up events in p+p (Au+Au) collisions are expected per triggered event. Preliminary study shows these pile-up events in p+p collisions can be easily distinguished from the hard scattering physics event of interest since these events are distributed in a wide z-vertex range over $|z| < 10$ cm, while the primary vertex can be reconstructed and well separated from others with a < 20 μm resolution. In the case of Au+Au collisions, the pile up will increase the overall detector hit occupancy. With the average 0.4 pile-up events, the occupancy in the innermost layer ($\sim 5 \times 10^7$ channels) will still be very low even in the central Au+Au collisions ($\sim$1500 particles per event). We expect that MVTX will also provide excellent space points matching to the INTT and the inner TPC which has a much longer integration time ($\sim$ 18 μs) than that of the MVTX. Full GEANT analysis framework to simulate the event pile-up effects on tracking is under development, more detailed studies with realistic detector simulation will be carried out soon.

6 Technical Scope and Deliverables

6.1 MAPS chips and stave production

We have reached an agreement with the ALICE ITS Upgrade Project management to produce the needed $\sim$1000 MAPS chips for the sPHENIX MVTX upgrade. These chips will be produced by Tower Jazz as part of the ALICE ITS Upgrade project. The MAPS chip complete QA will be carried out by the Korean institutions. sPHENIX stave mechanical carbon frames and connectors, which are identical to the ALICE ITS Upgrade Inner Barrel detectors, will be fabricated and tested using the ALICE ITS Upgrade facilities at CERN. sPHENIX collaboration will provide additional manpower, including students, postdocs and technicians, to help the stave assembly, mechanical survey and readout test in the CERN ITS/IB Upgrade labs. sPHENIX project will eventually obtain 68 fully tested staves from ALICE and assemble the final detector in the U.S., using the existing facilities at LBNL after the completion of the ALICE ITS mid-layer upgrade project.

6.2 Readout integration and testing

The MVTX readout electronics interfaces the MAPS staves and the sPHENIX DAQ, and also the trigger and slow control systems that monitor and record the status of MAPS chips. There are 48 staves in total (12/16/20 staves for layer 0/1/2, respectively). One Readout Unit (RU) is connected to one stave that contains 9 independent MAPS chips through 9 high-speed copper links. Each link is a point-to-point connection between RU and one MAPS chip, capable of data transmission speed 1.2 Gb/s. A total of 48 RUs are located about 5m away from the MVTX detector, in special 6U VME crates, the exact location of these crates is to be determined later. Data collected by RUs will be sent out through optical fibers to the Common Readout Units (CRU) in the sPHENIX Counting House (CH). The current readout plan is to use the ALICE RU for the stave readout, and modify the ALICE CRU firmware to reformat the data according to the sPHENIX specifications. The R&D effort of the MVTX-sPHENIX readout integration will be carried out by the LANL LDRD project. Figure 13) shows the readout chain of the MVTX system in sPHENIX.

To mitigate potential technical and schedule risks in the ALICE CRU development, we are also exploring other options to integrate the MVTX readout into the sPHENIX DAQ system. An interesting alternative DAQ back-end option to CRU is the FELIX PCIe card [23], which is designed as a high-throughput interface card with front-end and trigger electronics in the ATLAS Upgrade framework and is also considered as an

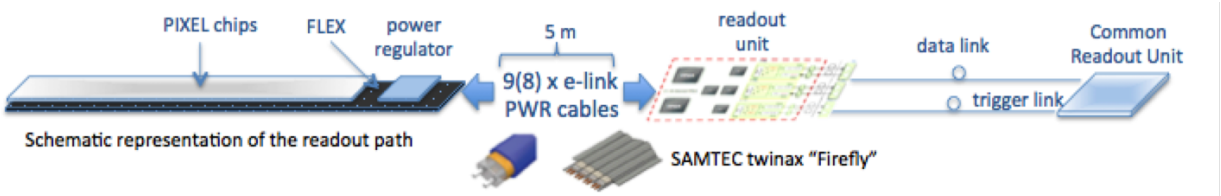

Figure 13: MVTX readout chain in sPHENIX. Readout Units are located about 5m from the MVTX, MAPS data are sent from RUs to CRUs in the Counting House through high-speed fiber optic links.

option for sPHENIX TPC readout. FELIX PCIe card provide comparable specification when compared with CRU, including 48-bidirectional GBT link to front-end, PCIex16-Gen3 interface to the hosting server for data output, and a large Xilinx 7-Series Kintex Ultrascale FPGA. The prototype FELIX card is available for testing and a production system is planned to be delivered to ALICE phase-I upgrade at the end of 2018, which also matches the R&D and production need for the sPHENIX MVTX detector.

6.3 Mechanical carbon structures

A description of the carbon fiber mechanical structures for the sPHENIX MVTX detector is provided in this chapter. The mechanical structures developed for the ALICE ITS Upgrade Inner Barrel are compatible with the general sPHENIX detector infrastructure and constraints with small modifications. In this proposal, the ITS Upgrade mechanics design will be used as the baseline for the sPHENIX MVTX detector mechanics. The design will be reviewed and adapted at LANL. The detector and service support carbon fiber structures will be fabricated at LBNL.

After discussing the requirements in Sec. 6.3.1, the mechanical structure that supports the Staves in layers is illustrated in Sec. 6.3.2, while Sec. 6.3.3 describes the cable routing to the Staves through the service barrels.

6.3.1 General requirements

The layout of the sPHENIX MVTX detector mechanical structure has been developed to fulfill the following design criteria:

- minimize material in the sensitive region;
- ensure high accuracy in the relative position of the detector sensors;
- provide an accurate position of the detector with respect to the TPC and the beam pipe;
- locate the first detector layer at a minimum distance to the beam pipe wall;
- ensure structure thermo-mechanical stability in time;
- facilitate accessibility for maintenance and inspection;
- facilitate assembly and disassembly of the detector layers and Staves.

The main mechanical support structure of the sPHENIX MVTX detector has the shape of a barrel. It holds in position the three detector layers. The barrel is divided into two halves, top and bottom, which are mounted separately around the beam pipe. The barrel is composed of a detector section and a service section. The Staves are housed in the detector barrel and are connected via electrical signal connections and power cables to patch panels. The patch panels are located immediately outside of the TPC. The service barrel

integrates the cable trays that support the signal and power cables through their routes from the detector Staves to the patch panels. Pipes that connect the vertex on-detector cooling system to the cooling plant in the sPHENIX hall are also routed through the service barrels.

6.3.2 Detector support structure

The main structural components of the detector barrels are the end-wheels and the Cylindrical and Conical Structural Shells (CCSS).

The end-wheels, which are light composite end-rings, ensure the precise positioning of the Staves in a layer. They provide the reference plane for fixing the two extremities of each Stave. Staves are positioned on the reference plane by two connectors that engage a locating pin fixed in the end-wheels at both ends. The Stave position is then frozen by a bolt that passes through the end-wheels and is screwed inside the connectors. This system ensures accurate positioning, within 10 m, during the assembly and provides the possibility to dismount and reposition the Stave with the same accuracy in case of maintenance. The end-wheels on the front side also provide the feed-through for the services. The different layers are connected together to form the barrel. An outer cylindrical structural shell (CYSS) connects the opposite end-wheels of the barrel and avoids that external loads are transferred directly to the Staves (see Figure 14). In order

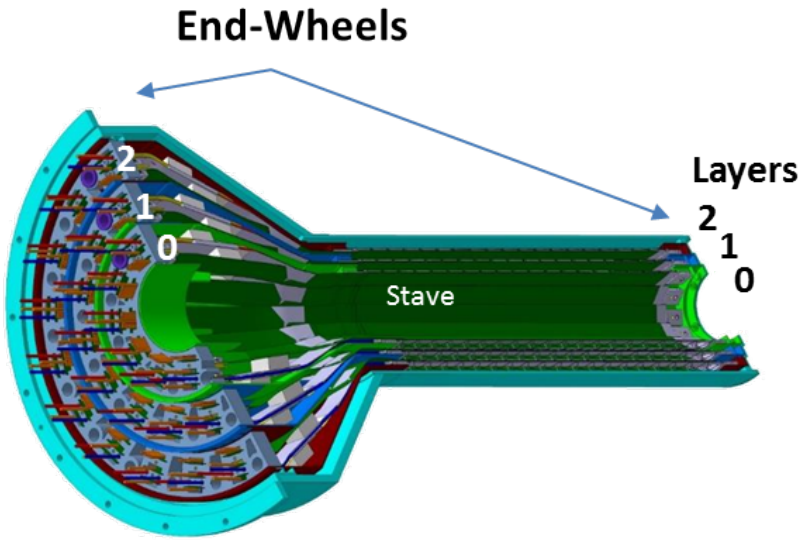

Figure 14: MVTX Half-Barrel, with the three half-layers fixed to the end-wheels. The layout shown here is based on the ALICE ITS Upgrade Inner Barrel design.

to minimize the material budget in the detection area and to facilitate installation and removal, the barrel is conceived as a cantilever structure supported at one end. A full scale prototype has been developed to verify the production process and the assembly procedure.

6.3.3 Service support structure

The service support structure design will be adapted from the ITS Upgrade Conical Support Shell (COSS) (see Figure 15) to match the sPHENIX TPC and general detector dimensions. The services attached to the detector barrel must be inserted or retracted together with the detectors. All services, including cooling pipes, power, and signal cables, will be integrated into the service barrel, which is an extension of the detector barrel. Power cables will be grouped with the cooling tubes in the service barrel in order to remove the heat they generate. The services layout will follow the detector modularity. The services will

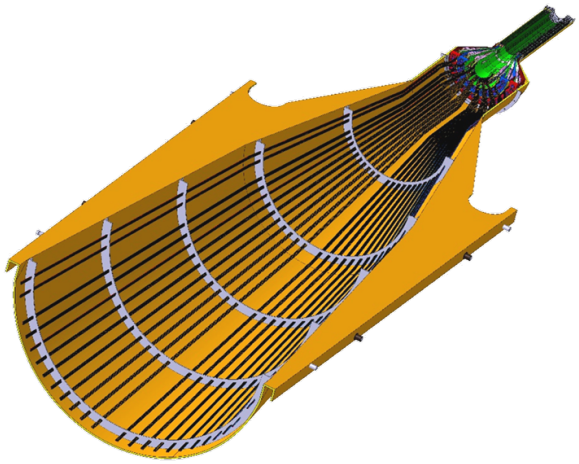

Figure 15: Conical Support Shell (COSS) forming the service half-barrel. The service barrel is an extension of the detector barrel and integrates all services, including cooling pipes, power, and signal cables. The layout shown here is based on the ALICE ITS Upgrade Inner Barrel design. It will be adapted to match the sPHENIX TPC and general detector dimensions.

be grouped per detector half-barrel and routed from the detector to a patch panel located in an accessible area outside the TPC on the TPC service support wheels. Inside the TPC, the service barrels will form a half-cone, jutting from the MAPS detector to the TPC service support wheel. The assembly composed of half detector barrel and half service barrel is inserted or extracted from the TPC bore by means of two sets of lateral rollers fixed on the barrels and sliding on their corresponding rails provided by the cage. The service barrel itself is a light composite structure that has to provide both structural stiffness and dimensional stability, to guarantee a precise installation of the sPHENIX MVTX detector inside the TPC.

6.4 Mechanical integration

The sPHENIX collaboration has plans to use a MAPS-based vertex detector similar to that used in the ALICE detector at the LHC. MIT will be working on the integration of this new detector into the current PHENIX detector at Brookhaven. MIT will work closely with the other detector groups in integrating the MAPS detector into sPHENIX. The support system used in the ALICE version of this detector was cantilevered but this constraint doesnt exist in the PHENIX design. This gives MIT flexibility in design of the new support system for the MAPS. The geometry of sHENIX will also require a new design for the services wheel which in principal can also be part of the support system. The service wheel will have to accommodate support and organization of the power and signal cables as well as the cooling tubes for each stave. There will also have to be accommodations for positioning and alignment of the detector as well as adequate fiducialization to allow for final survey. The current design of the detector also includes air cooling of some components which will also have to be incorporated into the design of the end wheels. MIT will work with the carbon fiber group at Berkeley as well as the group at CERN producing the staves to accomplish all of these goals. An extensive testing plan will need to be put in place to ensure that the final assembly will function as required. MIT will also work closely with the Min Bias and INTT groups to ensure that choices made early in the design cycle will integrate smoothly with their detectors and systems in the spectrometer.

MIT will lead the design in the cooling system for the staves. The current thought is to use a sub

atmospheric water system. This will be similar to the system used for the ALICE MAPS Vertex Tracker adapted for the sPHENIX MVTX configuration. This design is being considered so that if you have a leak in the system water doesnt drip onto the other detectors and damage them as sPHENIX has multiple barrel detectors. MIT will use CFD analysis to ensure that cooling system will be adequate for the staves. Figure 16 shows the proposed integrated mechanical support system of the MVTX.

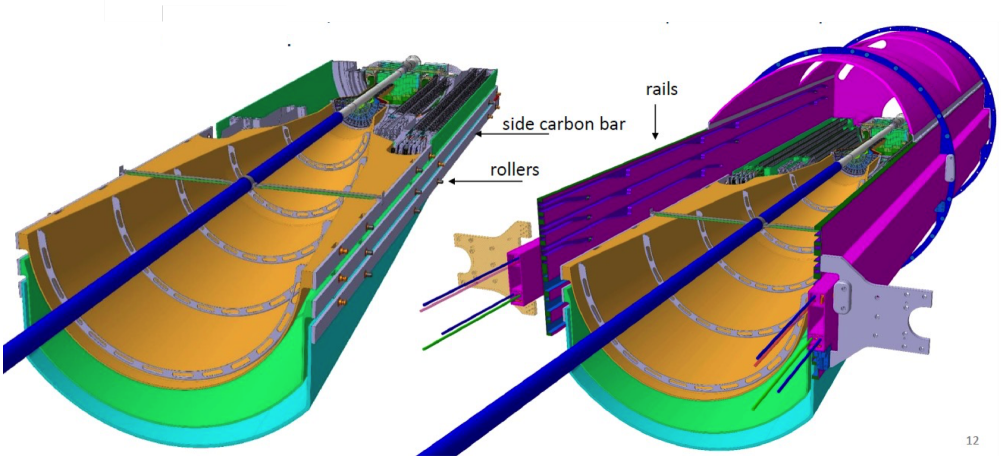

Figure 16: Basic structure of the the sPHENIX MAPS Vertex Detector mechanical supporting system.

6.5 Power System

The power system for the sPHENIX MVTX is included in the scope of participation of LBNL. LBNL is currently developing the power system for the ALICE ITS Upgrade. The prototypes are being currently tested and the production boards are being designed. The system meets the current sPHENIX MVTX detector requirements and its flexible design can be easily adapted to further needs. A brief description of requirements, architecture and main components is reported in this chapter.

6.5.1 Power system requirements

The requirements for the powering system (PS) are closely inter-dependent with the sensor and module FPC requirements, and with the detector environmental and operating conditions. These are most succinctly expressed as:

- Supply power (sensor supply and bias) to the staves such that:
  - Module sensor efficiency $\geq 99\%$
  - Module sensor noise rate $< 10^{-6}$
- Tolerate the radiation environment at the power board location.
- Interface to the RDO board for control of PS functions and readout of parameters.
- Fit into the space allocated in the vertex detector integration envelopes.

This design will be tested in the development of the staves for the ALICE ITS Upgrade and optimized for sPHENIX. The desirable functional attributes for system include:

- Overcurrent protection for each power channel

- Remote current readout for each power channel
- Remote voltage readout for each power channel
- Remote voltage setting capability for each channel

These attributes will allow for the protection of the sensors from damage due to latch-up conditions and, should there be any damage that increases current draw, to adjust the voltage to bring the sensors back into the operating voltage envelope.

6.5.2 Power system architecture

The structure of the power system is shown schematically in Figure 17. In this diagram, the main power

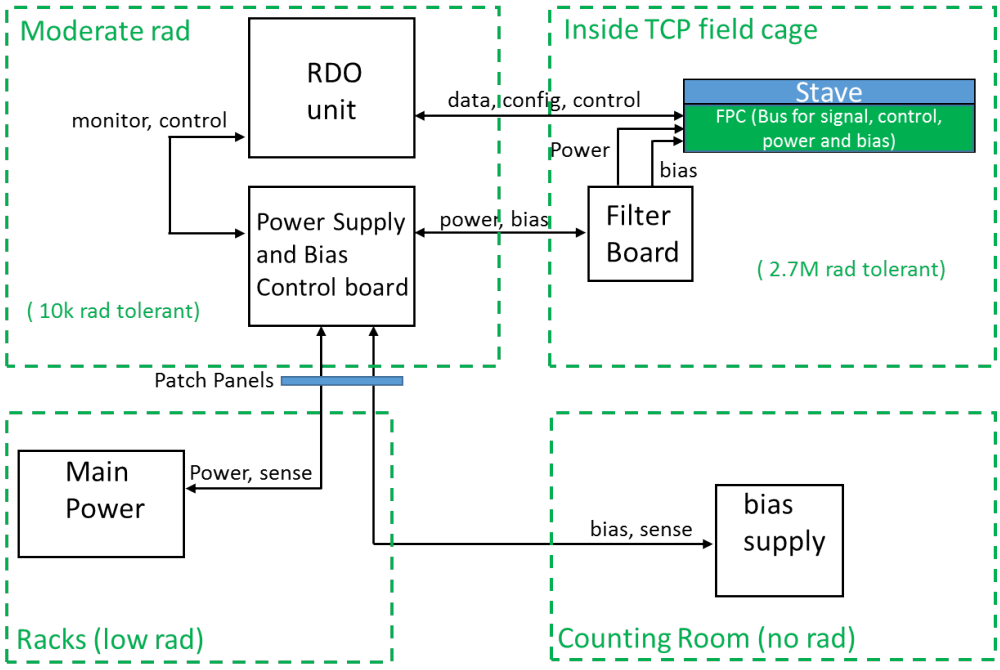

Figure 17: Basic Structure of the sPHENIX MVTX Vertex detector power system. Note the expected radiation load for each architecture block

supplies are expected to be located in low-radiation environment, tens of meters far from the interaction point. The main power supplies are expected to be CAEN mainframes populated with A3009/A3009HPB radiation tolerant CAEN power modules located in the racks in the hall. The back bias power supplies are expected to be CAEN mainframes populated with A2518 CAEN power modules located in the sPHENIX Counting House. All other boards shown are custom designs. The power supply and control board (PSCB) are being developed for the ALICE ITS Upgrade. They will contain the radiation tolerant power regulators, shunt resistors, overcurrent protection circuitry, current and voltage measuring circuitry and remote voltage setting circuitry. This set of boards will be located adjacent to the RDO crates at a larger radial distance and in a lower radiation. The primary function of the filter boards is to provide sufficient capacitive filtering to provide a well-regulated supply voltage to the power bus and sensor modules. This architecture is shown in Figure 18).

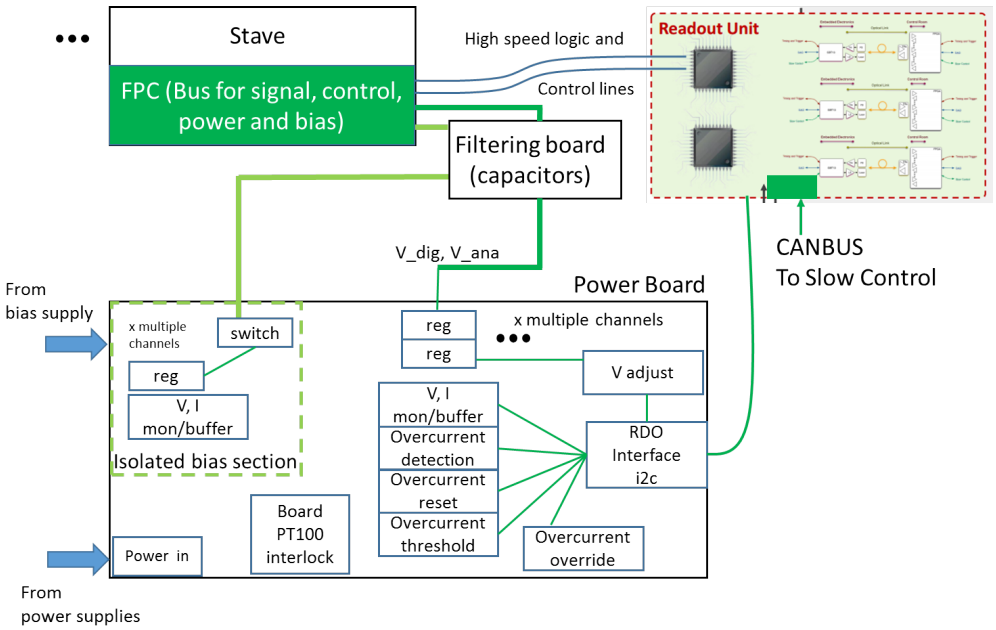

Figure 18: Basic architecture of the power board

6.6 MAPS stave assembly and testing at CERN

Following the completion of the ALICE ITS/IB assembly, experienced CERN techs will continue working on stave assembly for the sPHENIX MVTX project, using the same automated chip mounting machines at ALICE ITS/IB assembly labs. Students and postdocs from sPHENIX collaboration will work with CERN techs to perform the QA of the assembled staves, including visual inspection, test the stave readout at full speed on the test bench, analyze test data to quantify the quality and performance of the staves and produce QA traveler for each stave. Fully tested staves will be sent to LBNL to make half barrels.

6.7 Detector assembly

The scope of participation of LBNL in the sPHENIX MVTX detector includes also the assembly of the staves into the half detector support structure. The three layers, starting from the innermost one, consist of 12, 16 and 20 staves, respectively. Each stave is approximately 29 cm in length and contains nine Pixel Chips in a row connected to the FPC, which embeds signal, control, power and bias lines. The staves will be fabricated at CERN, as described in Sec. 6.6, and shipped to LBNL. The assembly scope of work will consist of:

1. Inspection, functional testing and validation of received staves
2. Metrology survey of the staves
3. Mounting of the staves onto the end-wheels to form the layers
4. Functional testing and validation of the layers
5. Metrology survey on the layers
6. Assembly of the three layers together and to the cylindrical support into the half detector

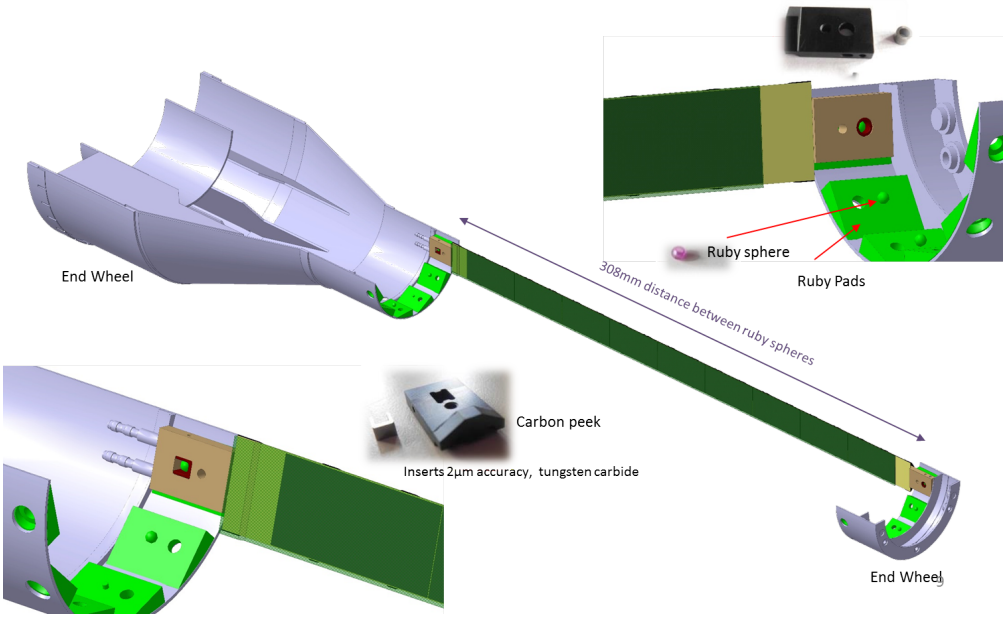

Figure 19: Stave assembly into layer

7. Functional testing and validation of the assemblies
8. Metrology survey on the final assemblies
9. Packing and shipment of the final assemblies to BNL.

The testing system is being developed by the ALICE Collaboration and is based on the ALICE RDO system. After the initial test, the stave is positioned on the end wheels reference planes by connectors at both extremities that engage a ruby sphere fixed in the reference plane (see Figure 19). The Stave position is then fixed by a bolt. The front side end-wheel includes the service barrel conical extension to hold and route all services, including cooling pipes, power, and signal cables. The three layers are assembled together and to the half detector CYSS, and the relative position is achieved by reference pins (see Figure 20). After each assembly step the assemblies are tested for validation and reworked if necessary, and a metrology survey is performed. The half detectors are finally ready to be packed and shipped to BNL.

6.8 Online software and Trigger

The online software for the MVTX will be part of the sPHENIX data acquisition (DAQ). The sPHENIX DAQ closely follows the design of the PHENIX DAQ [24]. The architecture is a fully pipelined design, which allows the next event to be triggered without waiting for the previous event to be fully processed. The existing PHENIX design allows for a depth of 4 such events to be buffered in front end modules before transmission. This multi-event buffering is the key concept to achieve the design event rate of 15 kHz while preserving livetime.

Figure 21 shows a schematic overview of the trigger, the front-end and the back-end systems. The Global Level 1 (GL1) system provides the trigger to the Master Timing Module (MTM), which is then distributed to the Granule Timing Modules (GTM). These GTMs provide the subsystem-specific trigger signals and

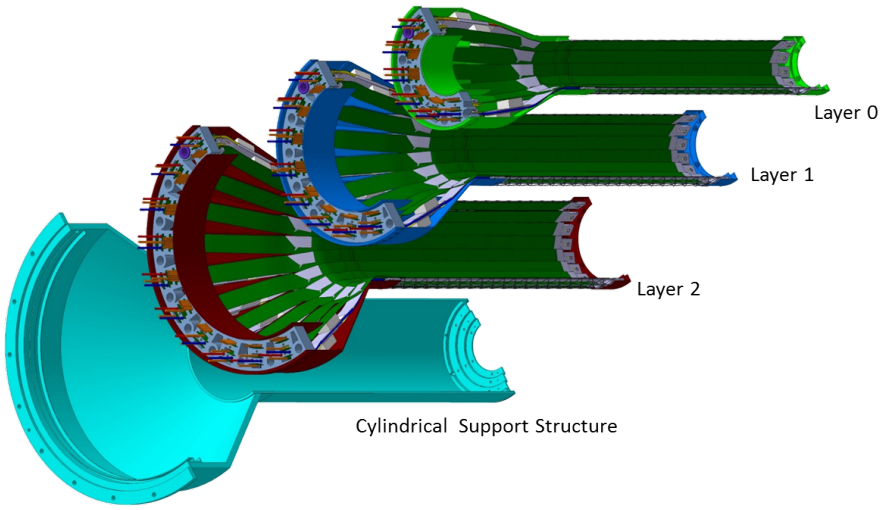

Figure 20: Layer assembly into half detector

timing to the MVTX Front End Modules (FEM). The data selected by the trigger system flow from the FEMs to Data Collection Modules (DCMs). Only the latest generation of the data collection module, the DCM-II, will be used. The DCM-IIs, which were developed for the PHENIX silicon vertex detectors, run detector-specific FPGA code to zero-suppress and package the data. This provides the freedom to change the data format as necessary by loading a new version of the FPGA code. A DCM-II has inputs for 8 data fibers. A group of DCM-IIs interface with the commodity computers called Sub-Event Buffers (SEBs) via

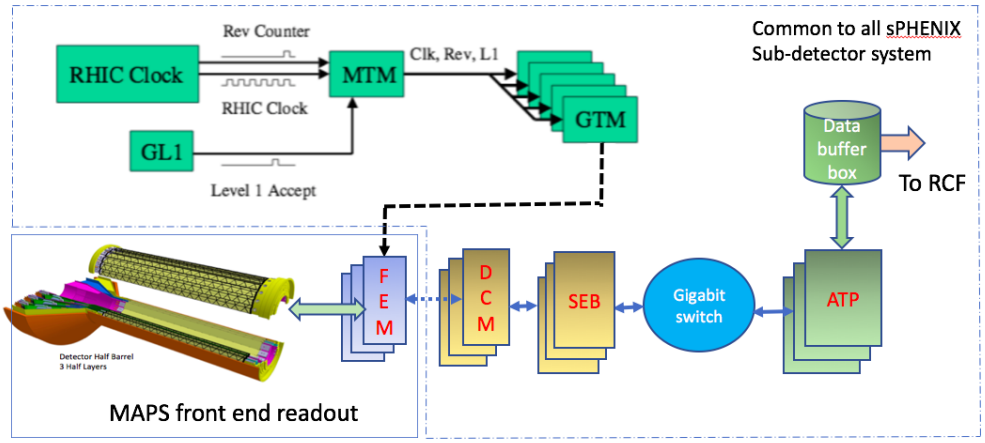

Figure 21: Online readout architecture for MAPS.

1.6 GBit/s serial optical links through a custom PCIe interface card, the JSEB-II. Due to overhead in the data encoding, the effective bandwidth through the fiber is 1.28 GBit/s. This 4-lane PCIe card is capable of sustaining 500 MB/s input into the SEB. This bandwidth is needed to achieve the envisioned event rate of about 15kHz. Each SEB only holds a fragment of the data of a given collision, which have to be combined together with data fragments from other sPHENIX detectors into a full event. This is accomplished on

computers called Assembly and Trigger Processors (ATPs) as shown in Fig. 21.

Other options could include the adaption of the LHCb/ALICE CRU or ATLAS FELIX as shown in 22, as proposed for the sPHENIX TPC readout.

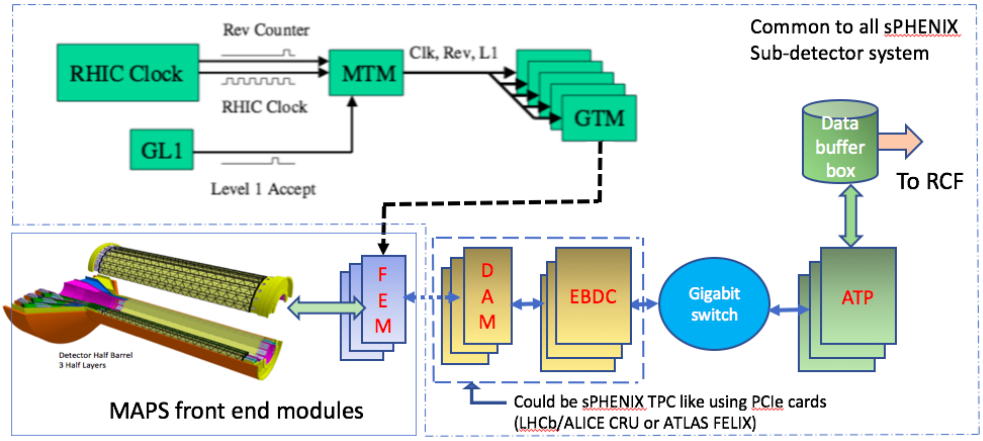

Figure 22: Online readout architecture for MAPS using PCIe cards.

6.9 Offline software - detector simulation, geometry, offline tracking

In sPHENIX, tracking simulation and reconstruction is performed in a global software framework including all tracking subsystems, inner pixel vertex detector (MVTX), intermediate silicon strip detector (INTT) and the outer time projection chamber (TPC).

- The sPHENIX software framework provide a custom-designed unified platform for detector simulation, raw data decoding, reconstruction and analysis. It has been successfully used in data analysis and simulation for the PHENIX collaboration in the past decade.
- The GEANT4 simulation toolkit [25] is employed to simulate interaction between collision product and full sPHENIX detector package and MVTX. MVTX group has provided the detailed geometry description of the sensitive and passive materials of the detector system. The hit information from GEANT4 is digitized into detector hit.
- Adjacent hits in the MVTX is group into clustered and all clusters. We employ a 5-dimensional Hough transform to locate the helical hit patterns from tracks bending through the solenoid field.
- Clusters belong to the same track are fitted via a Kalman-filter-based generic track-fitting toolkit, GenFit2 [26], to extract track parameter of displacement at vertex and momentum vector at vertex.
- All tracks are input to a generic toolkit, RAVE [27], to find and fit locations of the primary and secondary vertexes.

The result information is made available for analysis through the sPHENIX software framework, which produced the preliminary performance simulation studies as discussed in Section. 5. This software ecosystem will be continually developed and updated for simulation and data analysis for the proposed MVTX detector.

7 Organization and Collaboration

This is the list of the current collaborating Institutions and their focus areas:

Los Alamos National Lab (LANL) : Readout electronics and mechanics integration.

Lawrence Berkeley National Lab (LBNL) : Carbon structure, production, LV and HV power system, full detector assembly and test.

Brookhaven National Lab (BNL) : System integration and services, safety and monitoring.

Massachusetts Institute of Technology (MIT/Bates) : Mechanical system integration and cooling.

Massachusetts Institute of Technology (MIT) : Stave assembly and testing at CERN.

University of Texas at Austin (UT Austin) : MVTX readout electronics integration and testing.

University of Colorado : *b*-jet simulations and future hardware.

Iowa State University (ISU) : Detector assembly and testing, simulations.

Florida State University (FSU) : Offline and simulations.

University of New Mexico (UNM) : LV cabling & connectors.

New Mexico State University (NMSU) : Tracking algorithm and physics simulations.

Georgia State University (GSU) : Online software and trigger development.

University of California at Los Angeles (UCLA) : Simulation and readout testing.

University of California at Riverside (UCR) : Detector assembly and testing, simulations.

Yonsei University (Korea) : MAPS chips QA and readout, simulations

RIKEN/RBRC (Japan) : Mechanical integration, cooling, cabling, simulation, patter recognition.

Purdue: Detector assembly and testing, analysis. Silicon lab available.

Central China Normal University (CCNU/China): MAPS chip and stave test at CERN and/or CCNU.

Univ. of Science and Technology of China (USTC/China): MAPS chip and stave test, simulations.

Figure 23 shows the organization chart and tasks assigned for each Institution.

Detector R&D is underway at Los Alamos National Lab utilizing the granted internal LDRD funding (5M$ over 3 years). This R&D aims the assembly of a prototype with four staves and the full readout electronics chain needed to comply with the sPHENIX DAQ. LANL will work closely with UT-Austin and BNL groups on the final MVXT readout system design and production. The LANL LDRD project will also develop the initial design of the mechanical integration of the MVTX in the sPHENIX. MIT Bates Center will lead the final mechanical integration effort and has designated 0.25 FTE for an engineer and 1 FTE for a technician to work on the mechanical integration. LBNL will lead the effort of carbon structure fabrication, detector assembly and system readout test, and the production of the LV and HV power distribution boards and control system. Other institutions will help on various key tasks according to their available resources and expertise.

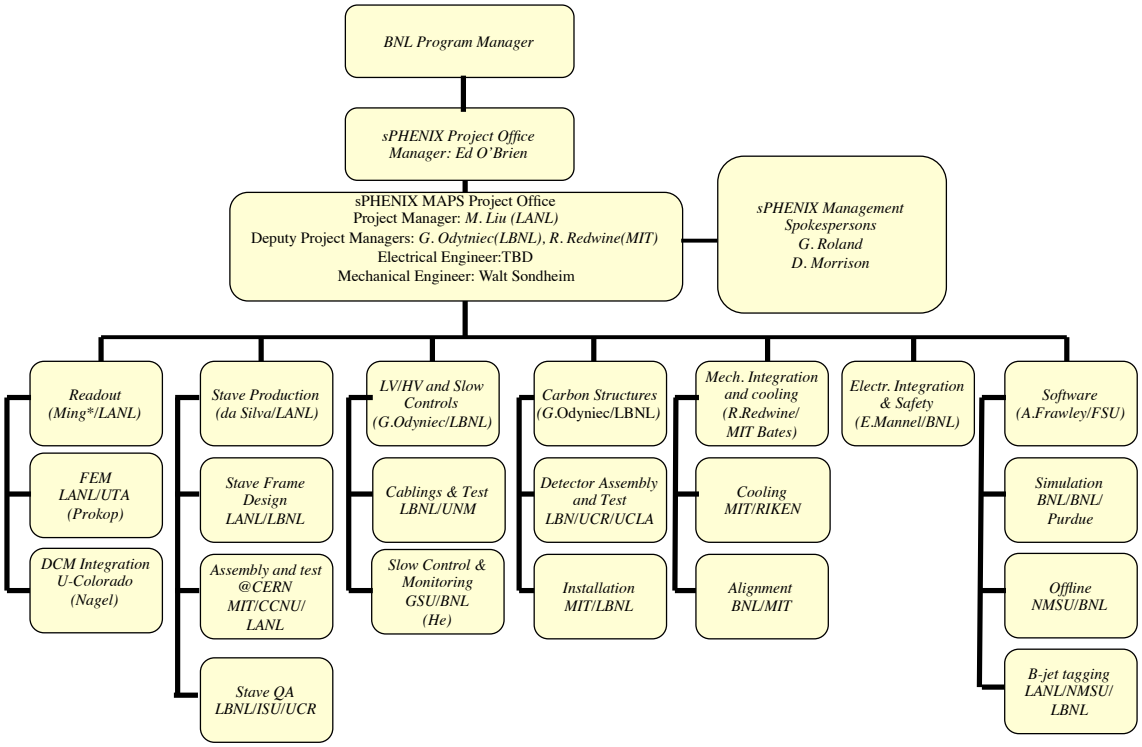

Figure 23: Organization chart of the MVTX project.

8 Schedule and Cost Baseline

8.1 Introduction

The MVTX project for sPHENIX relies an the fact that much of the conceptual design, prototype design, and prototyping has/will be done by the ALICE group at CERN and through a Los Alamos National Laboratory LDRD(Laboratory Directed research and Development) development effort. The cost and schedule for the is proposed for DOE/BNL support consists of final design efforts, procurement, assembly and installation. Presented here will be the proposed effort for the DOE/BNL portion. The complete cost and schedule file including the ALICE and LDRD effort is found in the appendix. The total project cost is \$4.9M after $\sim 30\%$ contingency applied. Projected finish date is the 4th Quarter of 2021.

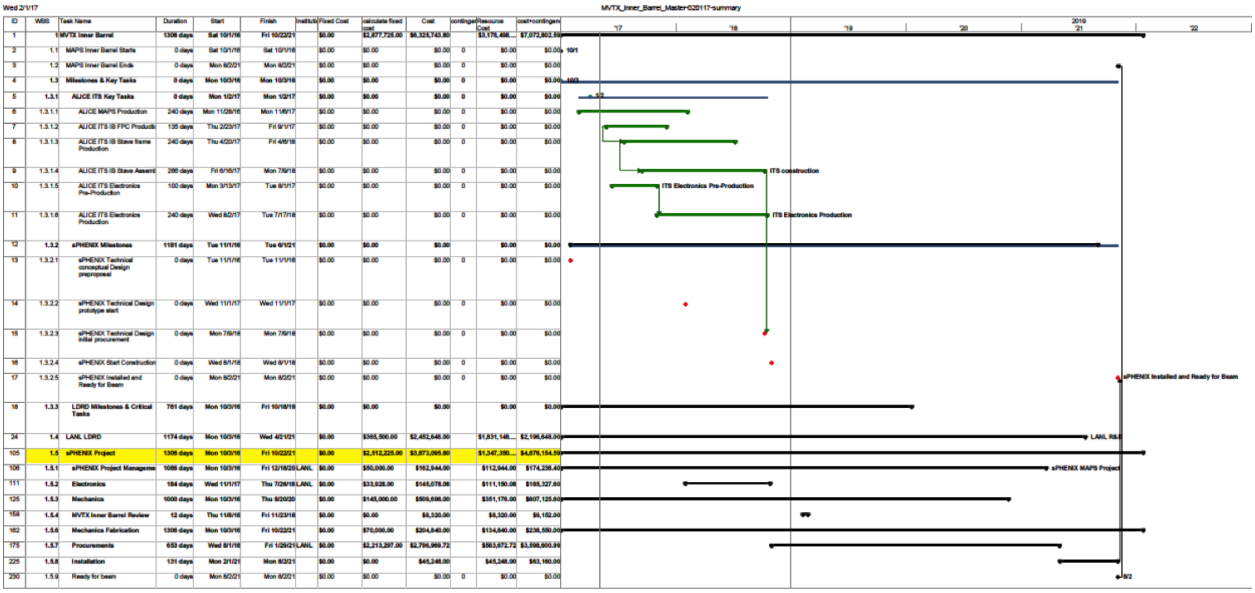

Figure 24: MVTX High Level Cost and Schedule.

8.2 Schedule

Fig. 24 is a high level view of the Cost and Schedule Gantt chart showing ALICE milestones that constrain the scheduling of the MVTX effort. The MVTX start date for the start of the technical design is in the 1st quarter of FY 2018, start construction is in the 4th quarter of FY 2018, installation and ready for beam is in the 3rd quarter of FY 2021.

An important constraint on this schedule is the production activities at ALICE. To reduce the MVTX project cost it is important that we are able to take advantage of the production lines at CERN. The Cost and Schedule is designed to use the CERN personnel and production lines at CERN. By doing this MVTX project does not have to implement a completely new production facility in the US with the necessary equipment, clean facilities, jigs, infrastructure, and personnel training that would be necessary. Currently, the end of ALICE production is in the 3rd quarter of FY 2018. Negotiations with CERN/BNL will be needed to accomplish the beginning of MAPS stave production at that time.

8.3 Cost

The cost of items in the Cost and Schedule are derived from actual ALICE costs and scaled by the number of staves. Since in the stave production cost at CERN, labor costs are not included, we have included

a separate task under procurements to provide for our use of the CERN personnel in producing our staves. Electronics costs are based on obtaining Gerber files from ALICE and fabricating them in the US. This was done previously for the mini-CAPTAIN LANL LDRD with great success. Costs were based on the board complexity and applied to the MVTX electronics. The cost of the common readout board which will be designed at LANL is based on a similarly complex board that was recently fabricated for the FVTX detector at PHENIX. Mechanical procurements costs are based on ALICE procurements of the same item. The mechanical design of the MVTX detector will be a replication of the ALICE design but since the MVTX detector will sit inside the Intermediate Tracker which is not yet designed we have included a 50% contingency to cover a possible redesign. Mechanical Integration into sPHENIX requires a clear definition of the surrounding systems. Unfortunately, because the inner volume is still in a state of flux, we have looked at the global support structure for the TPC as an estimate for our needs but with a large contingency. Contingency is risked based and varies between 25% and 50%.

8.4 Resources

The level of resources is based on previous experience in other projects such as FVTX, ALICE, and PHENIX. Resource costs are institution specific with fully costed hourly rates used.

8.5 Milestones

Here are the milestones of the project.

Table 3: Milestones

Milestones	Time
MVTX Preproposal finish	4th Qtr FY 2017
MVTX Proposal Review	2nd Qtr FY 2018
Stave Procurement	4th Qtr FY 2018
Start Construction	4th Qtr FY 2018
Installation	1st Qtr FY 2021
Ready for Beam	4th Qtr FY 2021

8.6 Major Cost Items

Here we list the cost of major items.

Table 4: Major Cost Items

WBS	Task Name	Cost (K)	Cost with Contingency (K)
1.5.7.1.1	Produce 68 staves	$650	$880
1.5.7.1.2	CERN Manpower	$500	$680
1.5.7.2.1	Readout Units(RDO)	$290	$360
1.5.7.2.2	Optical Links	$83	$100
1.5.7.2.3	Common Readout Units(CRU)	$180	$230
1.5.7.2.4	CRU Contingency	$90	$110
1.5.7.2.16	Service Half Barrels	$120	$150

End of proposal narrative; supplemental materials to follow.

9 Project Timeline, Deliverables, and Tasks

Here is the detailed Cost and Schedule information.

ID	WBS	Task Name	Duration	Start	Finish	Institutic	Fixed Cost	calculate fixed cost	Cost	contingen	Resource Cost	cost+contingen
1	**1**	**MVTX Inner Barrel**	**1306 days**	**Sat 10/1/16**	**Fri 10/22/21**		**$0.00**	**$2,877,725.00**	**$6,325,743.80**		**$3,178,498....**	**$7,072,802.59**
2	1.1	MAPS Inner Barrel Starts	0 days	Sat 10/1/16	Sat 10/1/16		$0.00	$0.00	$0.00	0	$0.00	$0.00
3	1.2	MAPS Inner Barrel Ends	0 days	Mon 8/2/21	Mon 8/2/21		$0.00	$0.00	$0.00	0	$0.00	$0.00
4	**1.3**	**Milestones & Key Tasks**	**0 days**	**Mon 10/3/16**	**Mon 10/3/16**		**$0.00**	**$0.00**	**$0.00**	**0**	**$0.00**	**$0.00**
5	**1.3.1**	**ALICE ITS Key Tasks**	**0 days**	**Mon 1/2/17**	**Mon 1/2/17**		**$0.00**	**$0.00**	**$0.00**	**0**	**$0.00**	**$0.00**
6	1.3.1.1	ALICE MAPS Production	240 days	Mon 11/28/16	Mon 11/6/17		$0.00	$0.00	$0.00	0	$0.00	$0.00
7	1.3.1.2	ALICE ITS IB FPC Productic	135 days	Thu 2/23/17	Fri 9/1/17		$0.00	$0.00	$0.00	0	$0.00	$0.00
8	1.3.1.3	ALICE ITS IB Stave frame Production	240 days	Thu 4/20/17	Fri 4/6/18		$0.00	$0.00	$0.00	0	$0.00	$0.00
9	1.3.1.4	ALICE ITS IB Stave Assemb	266 days	Fri 6/16/17	Mon 7/9/18		$0.00	$0.00	$0.00	0	$0.00	$0.00
10	1.3.1.5	ALICE ITS Electronics Pre-Production	100 days	Mon 3/13/17	Tue 8/1/17		$0.00	$0.00	$0.00	0	$0.00	$0.00
11	1.3.1.6	ALICE ITS Electronics Production	240 days	Wed 8/2/17	Tue 7/17/18		$0.00	$0.00	$0.00	0	$0.00	$0.00
12	**1.3.2**	**sPHENIX Milestones**	**1181 days**	**Tue 11/1/16**	**Tue 6/1/21**		**$0.00**	**$0.00**	**$0.00**		**$0.00**	**$0.00**
13	1.3.2.1	sPHENIX Technical conceptual Design preproposal	0 days	Tue 11/1/16	Tue 11/1/16		$0.00	$0.00	$0.00	0	$0.00	$0.00
14	1.3.2.2	sPHENIX Technical Design prototype start	0 days	Wed 11/1/17	Wed 11/1/17		$0.00	$0.00	$0.00	0	$0.00	$0.00
15	1.3.2.3	sPHENIX Technical Design initial procurement	0 days	Mon 7/9/18	Mon 7/9/18		$0.00	$0.00	$0.00	0	$0.00	$0.00
16	1.3.2.4	sPHENIX Start Construction	0 days	Wed 8/1/18	Wed 8/1/18		$0.00	$0.00	$0.00	0	$0.00	$0.00
17	1.3.2.5	sPHENIX Installed and Ready for Beam	0 days	Mon 8/2/21	Mon 8/2/21		$0.00	$0.00	$0.00	0	$0.00	$0.00
18	**1.3.3**	**LDRD Milestones & Critical Tasks**	**781 days**	**Mon 10/3/16**	**Fri 10/18/19**		**$0.00**	**$0.00**	**$0.00**		**$0.00**	**$0.00**
24	**1.4**	**LANL LDRD**	**1174 days**	**Mon 10/3/16**	**Wed 4/21/21**		**$0.00**	**$365,500.00**	**$2,452,648.00**		**$1,831,148....**	**$2,196,648.00**
105	**1.5**	**sPHENIX Project**	**1306 days**	**Mon 10/3/16**	**Fri 10/22/21**		**$0.00**	**$2,512,225.00**	**$3,873,095.80**		**$1,347,350....**	**$4,876,154.59**
106	**1.5.1**	**sPHENIX Project Manageme**	**1086 days**	**Mon 10/3/16**	**Fri 12/18/20**	**LANL**	**$0.00**	**$50,000.00**	**$162,944.00**		**$112,944.00**	**$174,238.40**
107	1.5.1.1	Project Manager	1086 days	Mon 10/3/16	Fri 12/18/20		$0.00	$0.00	$0.00	.10	$0.00	$0.00
108	1.5.1.2	Mechanical Integration Engineer	1086 days	Mon 10/3/16	Fri 12/18/20		$0.00	$0.00	$56,472.00	.10	$56,472.00	$62,119.20
109	1.5.1.3	Electronics Integration Engineer	1086 days	Mon 10/3/16	Fri 12/18/20		$0.00	$0.00	$56,472.00	.10	$56,472.00	$62,119.20
110	1.5.1.4	Travel	1000 days	Mon 10/3/16	Thu 8/20/20		$50,000.00	$50,000.00	$50,000.00	0	$0.00	$50,000.00
111	**1.5.2**	**Electronics**	**184 days**	**Wed 11/1/17**	**Thu 7/26/18**	**LANL**	**$0.00**	**$33,928.00**	**$145,078.08**		**$111,150.08**	**$185,327.60**
112	**1.5.2.1**	**Final Electronics Design**	**40 days**	**Fri 6/1/18**	**Thu 7/26/18**	**LANL**	**$0.00**	**$25,000.00**	**$63,400.00**		**$38,400.00**	**$83,230.00**
113	1.5.2.1.1	Produce RDU first unit	4 wks	Fri 6/1/18	Thu 6/28/18		$10,000.00	$10,000.00	$12,400.00	.25	$2,400.00	$15,500.00
114	1.5.2.1.2	Test RDU	2 wks	Fri 6/29/18	Thu 7/12/18		$0.00	$0.00	$11,200.00	.25	$11,200.00	$14,000.00
115	1.5.2.1.3	Produce CRU first unit	4 wks	Fri 6/1/18	Thu 6/28/18		$15,000.00	$15,000.00	$17,400.00	.35	$2,400.00	$23,490.00
116	1.5.2.1.4	Test CRU	2 wks	Fri 6/29/18	Thu 7/12/18		$0.00	$0.00	$11,200.00	.35	$11,200.00	$15,120.00
117	1.5.2.1.5	Final Electronics System Test	2 wks	Fri 7/13/18	Thu 7/26/18		$0.00	$0.00	$11,200.00	.35	$11,200.00	$15,120.00
118	**1.5.2.2**	**MAPS Power System**	**82 days**	**Wed 11/1/17**	**Tue 3/6/18**	**LBNL**	**$0.00**	**$8,928.00**	**$81,678.08**		**$72,750.08**	**$102,097.60**
119	**1.5.2.2.1**	**Power Boards**	**82 days**	**Wed 11/1/17**	**Tue 3/6/18**		**$0.00**	**$8,928.00**	**$81,678.08**		**$72,750.08**	**$102,097.60**
120	1.5.2.2.1.1	Review ALICE PB Design	20 days	Wed 11/1/17	Fri 12/1/17		$0.00	$0.00	$26,748.80	.25	$26,748.80	$33,436.00
121	1.5.2.2.1.2	Fabricate PB protype	30 days	Mon 12/4/17	Fri 1/19/18		$5,771.00	$5,771.00	$12,683.00	.25	$6,912.00	$15,853.75
122	1.5.2.2.1.3	Test PB Prototype	20 days	Mon 1/22/18	Fri 2/16/18		$1,154.00	$1,154.00	$24,194.00	.25	$23,040.00	$30,242.50
123	1.5.2.2.1.4	Design Production PB	10 days	Mon 2/19/18	Fri 3/2/18		$2,003.00	$2,003.00	$15,377.40	.25	$13,374.40	$19,221.75
124	1.5.2.2.1.5	Power System Review	2 days	Mon 3/5/18	Tue 3/6/18		$0.00	$0.00	$2,674.88	.25	$2,674.88	$3,343.60
125	**1.5.3**	**Mechanics**	**1000 days**	**Mon 10/3/16**	**Thu 8/20/20**		**$0.00**	**$145,000.00**	**$509,696.00**		**$351,176.00**	**$607,125.60**
126	**1.5.3.1**	**Mechanics Detector Design**	**200 days**	**Wed 11/1/17**	**Fri 8/17/18**	**LANL**	**$0.00**	**$25,000.00**	**$243,400.00**		**$218,400.00**	**$310,750.00**
127	1.5.3.1.1	Review ALICE design	2 wks	Wed 11/1/17	Wed 11/15/17		$0.00	$0.00	$10,400.00	.25	$10,400.00	$13,000.00
128	1.5.3.1.2	modify design if necessary	5 wks	Thu 11/16/17	Fri 12/22/17		$0.00	$0.00	$26,000.00	.30	$26,000.00	$33,800.00
129	1.5.3.1.3	Modify Service Barrel	5 wks	Mon 1/1/18	Fri 2/2/18		$0.00	$0.00	$26,000.00	.25	$26,000.00	$32,500.00

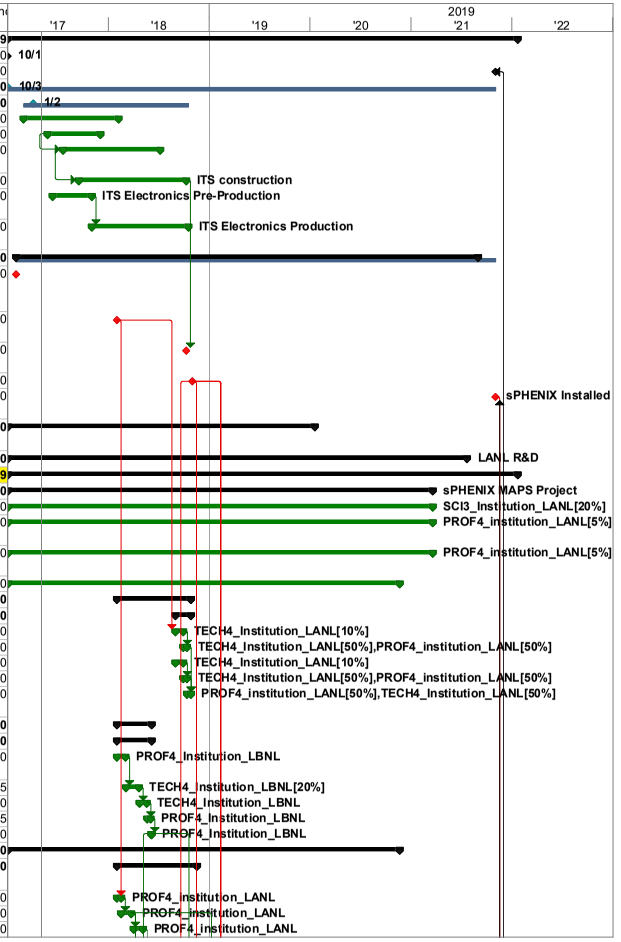

ID	WBS	Task Name	Duration	Start	Finish	Institutic	Fixed Cost	calculate fixed cost	Cost	contingen	Resource Cost	cost+contingen
130	1.5.3.1.4	design interface to rail system	5 wks	Mon 2/5/18	Fri 3/9/18		$0.00	$0.00	$26,000.00	.25	$26,000.00	$32,500.00
131	1.5.3.1.5	Develop MAPS inner tracker mechanical model	1 mon	Mon 3/12/18	Fri 4/6/18		$0.00	$0.00	$20,800.00	.25	$20,800.00	$26,000.00
132	**1.5.3.1.6**	**Stave Support Frame & Global Interface to sPHENIX**	**165 days**	**Mon 1/1/18**	**Fri 8/17/18**		**$0.00**	**$25,000.00**	**$134,200.00**		**$109,200.00**	**$172,950.00**
133	1.5.3.1.6.1	Design Interface to sPHENIX	50 days	Mon 1/1/18	Fri 3/9/18		$0.00	$0.00	$52,000.00	.35	$52,000.00	$70,200.00
134	1.5.3.1.6.2	FEA,Thermal, stress analysis	30 days	Mon 3/12/18	Fri 4/20/18		$0.00	$0.00	$31,200.00	.25	$31,200.00	$39,000.00
135	1.5.3.1.6.3	prototype	60 days	Fri 4/20/18	Fri 7/13/18		$25,000.00	$25,000.00	$25,000.00	.25	$0.00	$31,250.00
136	1.5.3.1.6.4	test	10 days	Mon 7/16/18	Fri 7/27/18		$0.00	$0.00	$10,400.00	.25	$10,400.00	$13,000.00
137	1.5.3.1.6.5	final design	15 days	Mon 7/30/18	Fri 8/17/18		$0.00	$0.00	$15,600.00	.25	$15,600.00	$19,500.00
138	**1.5.3.2**	**Mechanics Integration**	**1000 days**	**Mon 10/3/16**	**Thu 8/20/20**		**$0.00**	**$120,000.00**	**$201,320.00**		**$81,320.00**	**$233,534.00**
139	1.5.3.2.1	Travel MIT	1000 days	Mon 10/3/16	Thu 8/20/20		$70,000.00	$70,000.00	$70,000.00	0	$0.00	$70,000.00
140	**1.5.3.2.2**	**Cooling System**	**25 days**	**Mon 8/20/18**	**Fri 9/21/18**	**MIT**	**$0.00**	**$20,000.00**	**$45,680.00**		**$25,680.00**	**$57,100.00**
141	1.5.3.2.2.1	Design (modify ALICE)	10 days	Mon 8/20/18	Fri 8/31/18		$0.00	$0.00	$12,320.00	.25	$12,320.00	$15,400.00
142	1.5.3.2.2.2	Mock up Testing	10 days	Mon 9/3/18	Fri 9/14/18		$20,000.00	$20,000.00	$27,200.00	.25	$7,200.00	$34,000.00
143	1.5.3.2.2.3	Final Desgin of Cooling System	5 days	Mon 9/17/18	Fri 9/21/18		$0.00	$0.00	$6,160.00	.25	$6,160.00	$7,700.00
144	**1.5.3.2.3**	**Safety Systems**	**40 days**	**Mon 9/24/18**	**Fri 11/16/18**	**MIT**	**$0.00**	**$10,000.00**	**$34,640.00**		**$24,640.00**	**$42,684.00**
145	1.5.3.2.3.1	review sensors & interlocks	10 days	Mon 9/24/18	Fri 10/5/18		$0.00	$0.00	$6,160.00	.15	$6,160.00	$7,084.00
146	1.5.3.2.3.2	cooling interlocks design	30 days	Mon 10/8/18	Fri 11/16/18		$10,000.00	$10,000.00	$28,480.00	.25	$18,480.00	$35,600.00
147	**1.5.3.2.4**	**Stave Assembly Tooling**	**45 days**	**Mon 8/20/18**	**Fri 10/19/18**	**LANL**	**$0.00**	**$20,000.00**	**$51,000.00**		**$31,000.00**	**$63,750.00**
148	1.5.3.2.4.1	design	10 days	Mon 8/20/18	Fri 8/31/18		$0.00	$0.00	$10,400.00	.25	$10,400.00	$13,000.00
149	1.5.3.2.4.2	prototype	30 days	Mon 9/3/18	Fri 10/12/18		$20,000.00	$20,000.00	$38,000.00	.25	$18,000.00	$47,500.00
150	1.5.3.2.4.3	final jig design	5 days	Mon 10/15/18	Fri 10/19/18		$0.00	$0.00	$2,600.00	.25	$2,600.00	$3,250.00
151	**1.5.3.3**	**Mechanics Final Design Review**	**13 days**	**Mon 10/22/18**	**Wed 11/7/18**		**$0.00**	**$0.00**	**$23,376.00**		**$9,856.00**	**$10,841.60**
152	1.5.3.3.1	Mechanical design review	2 days	Mon 10/22/18	Tue 10/23/18		$0.00	$0.00	$2,464.00	.10	$2,464.00	$2,710.40
153	1.5.3.3.2	Incorporate Review Comments	10 days	Wed 10/24/18	Tue 11/6/18		$0.00	$0.00	$6,160.00	.10	$6,160.00	$6,776.00
154	1.5.3.3.3	Complete Final Mechanical Design	1 day	Wed 11/7/18	Wed 11/7/18		$0.00	$0.00	$1,232.00	.10	$1,232.00	$1,355.20
155	**1.5.3.4**	**Ancillary Systems**	**40 days**	**Mon 1/1/18**	**Fri 2/23/18**		**$0.00**	**$0.00**	**$41,600.00**		**$41,600.00**	**$52,000.00**
156	1.5.3.4.1	Metrology design	20 days	Mon 1/1/18	Fri 1/26/18	LANL	$0.00	$0.00	$20,800.00	.25	$20,800.00	$26,000.00
157	1.5.3.4.2	Design jigs	20 days	Mon 1/29/18	Fri 2/23/18	LANL	$0.00	$0.00	$20,800.00	.25	$20,800.00	$26,000.00
158	**1.5.4**	**MVTX Inner Barrel Review**	**12 days**	**Thu 11/8/18**	**Fri 11/23/18**		**$0.00**	**$0.00**	**$8,320.00**		**$8,320.00**	**$9,152.00**
159	1.5.4.1	MVTX Final Design Review	1 day	Thu 11/8/18	Thu 11/8/18		$0.00	$0.00	$1,040.00	.10	$1,040.00	$1,144.00
160	1.5.4.2	Incorporate Review Comments	10 days	Fri 11/9/18	Thu 11/22/18		$0.00	$0.00	$5,200.00	.10	$5,200.00	$5,720.00
161	1.5.4.3	Complete Final Design	1 day	Fri 11/23/18	Fri 11/23/18		$0.00	$0.00	$2,080.00	.10	$2,080.00	$2,288.00
162	**1.5.6**	**Mechanics Fabrication**	**1306 days**	**Mon 10/3/16**	**Fri 10/22/21**		**$0.00**	**$70,000.00**	**$204,840.00**		**$134,840.00**	**$238,550.00**
163	1.5.6.1	Travel LBNL	1000 days	Mon 10/3/16	Thu 8/20/20		$70,000.00	$70,000.00	$70,000.00	0	$0.00	$70,000.00
164	**1.5.6.2**	**Support Structure Cylindrical Structural Shell(CYSS)**	**23 days**	**Wed 11/1/17**	**Wed 12/6/17**	**LBNL**	**$0.00**	**$0.00**	**$30,761.12**		**$30,761.12**	**$38,451.40**
165	1.5.6.2.1	Review ALICE CYSS Design	10 days	Wed 11/1/17	Wed 11/15/17		$0.00	$0.00	$13,374.40	.25	$13,374.40	$16,718.00
166	1.5.6.2.2	Review Design-Fabrication Compatibility	6 days	Thu 11/16/17	Mon 11/27/17		$0.00	$0.00	$8,024.64	.25	$8,024.64	$10,030.80
167	1.5.6.2.3	CYSS Review	7 days	Tue 11/28/17	Wed 12/6/17		$0.00	$0.00	$9,362.08	.25	$9,362.08	$11,702.60
168	**1.5.6.3**	**Service Conical Half Shell**	**27 days**	**Wed 11/1/17**	**Tue 12/12/17**	**LBNL**	**$0.00**	**$0.00**	**$36,110.88**		**$36,110.88**	**$45,138.60**
169	1.5.6.3.1	Review ALICE COSS Design	15 days	Wed 11/1/17	Wed 11/22/17		$0.00	$0.00	$20,061.60	.25	$20,061.60	$25,077.00

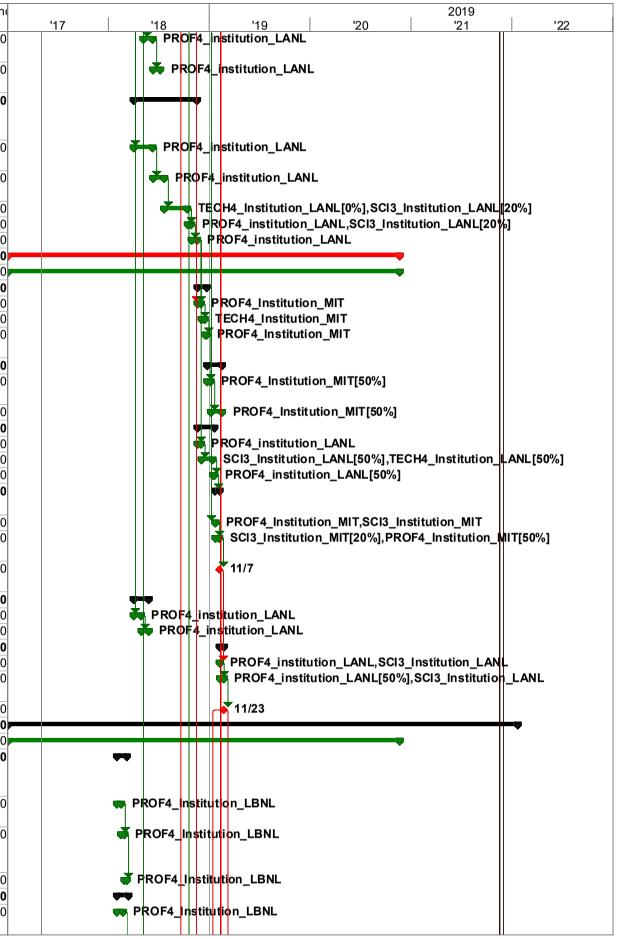

ID	WBS	Task Name	Duration	Start	Finish	Institutic	Fixed Cost	calculate fixed cost	Cost	continger	Resource Cost	cost+contingen
170	1.5.6.3.2	Review Design-Fabrication Compatibility	6 days	Mon 11/27/17	Mon 12/4/17		$0.00	$0.00	$8,024.64	.25	$8,024.64	$10,030.80
171	1.5.6.3.3	COSS Review	6 days	Tue 12/5/17	Tue 12/12/17		$0.00	$0.00	$8,024.64	.25	$8,024.64	$10,030.80
172	**1.5.6.4**	**Shipping and Storage Containers**	**59 days**	**Tue 8/3/21**	**Fri 10/22/21**	**LBNL**	**$0.00**	**$0.00**	**$67,968.00**		**$67,968.00**	**$84,960.00**
173	1.5.6.4.1	Design Storage Cabinets	39 days	Tue 8/3/21	Fri 9/24/21		$0.00	$0.00	$44,928.00	.25	$44,928.00	$56,160.00
174	1.5.6.4.2	Design Shipping Containe	20 days	Mon 9/27/21	Fri 10/22/21		$0.00	$0.00	$23,040.00	.25	$23,040.00	$28,800.00
175	**1.5.7**	**Procurements**	**653 days**	**Wed 8/1/18**	**Fri 1/29/21**	**LANL**	**$0.00**	**$2,213,297.00**	**$2,796,969.72**		**$583,672.72**	**$3,598,600.99**
176	**1.5.7.1**	**CERN Procurements**	**180 days**	**Fri 11/23/18**	**Fri 8/2/19**		**$0.00**	**$1,025,670.00**	**$1,235,794.80**		**$210,124.80**	**$1,652,546.50**
177	1.5.7.1.1	Produce 68 Inner Staves	180 days	Fri 11/23/18	Fri 8/2/19	BNL	$445,670.00	$445,670.00	$653,030.00	.35	$207,360.00	$881,590.50
178	1.5.7.1.2	Stave Production Full Cost Recovery of CERN Manpower	180 days	Mon 11/26/18	Fri 8/2/19		$500,000.00	$500,000.00	$500,000.00	.35	$0.00	$675,000.00
179	1.5.7.1.3	Other ITS/CERN Test Equiptment Items	120 days	Mon 11/26/18	Fri 5/10/19	LBNL	$30,000.00	$30,000.00	$32,764.80	.25	$2,764.80	$40,956.00
180	1.5.7.1.4	Travel and Per Diem at CERN	180 days	Mon 11/26/18	Fri 8/2/19	LANL	$50,000.00	$50,000.00	$50,000.00	.10	$0.00	$55,000.00
181	**1.5.7.2**	**Non-CERN Procurements**	**183 days**	**Wed 8/1/18**	**Fri 4/12/19**		**$0.00**	**$1,173,261.00**	**$1,248,940.20**		**$75,679.20**	**$1,561,175.25**
182	1.5.7.2.1	Procure 68 Readout /RDO Units	100 days	Mon 11/26/18	Fri 4/12/19	LANL	$265,740.00	$265,740.00	$289,740.00	.25	$24,000.00	$362,175.00
183	1.5.7.2.2	Procure Optical Links 68	60 days	Tue 11/27/18	Mon 2/18/19	LANL	$81,600.00	$81,600.00	$83,040.00	.25	$1,440.00	$103,800.00
184	1.5.7.2.3	Procure 34 Common Readout Units	100 days	Fri 8/3/18	Thu 12/20/18	LANL	$181,700.00	$181,700.00	$184,100.00	.25	$2,400.00	$230,125.00
185	1.5.7.2.4	sPHENIX CRU Production Contingency	100 days	Fri 8/3/18	Thu 12/20/18	LANL	$90,000.00	$90,000.00	$90,000.00	.25	$0.00	$112,500.00
186	1.5.7.2.5	Procure 100 SamTec Cables	60 days	Mon 8/6/18	Fri 10/26/18	LANL	$27,000.00	$27,000.00	$28,440.00	.25	$1,440.00	$35,550.00
187	1.5.7.2.6	Fab production PB	40 days	Thu 8/2/18	Wed 9/26/18	LBNL	$62,973.00	$62,973.00	$62,973.00	.25	$0.00	$78,716.25
188	1.5.7.2.7	Procure Power Supplies	50 days	Fri 8/3/18	Thu 10/11/18	LBNL	$48,015.00	$48,015.00	$49,167.00	.25	$1,152.00	$61,458.75
189	1.5.7.2.8	Procure Cooling Plant	100 days	Mon 8/6/18	Fri 12/21/18	MIT	$40,000.00	$40,000.00	$41,440.00	.25	$1,440.00	$51,800.00
190	1.5.7.2.9	Procure Assembly Fixtures & Jigs	60 days	Tue 8/7/18	Mon 10/29/18	LANL	$50,000.00	$50,000.00	$52,688.00	.25	$2,688.00	$65,860.00
191	1.5.7.2.10	Procure End Wheels from CERN	100 days	Wed 8/8/18	Tue 12/25/18	LBNL	$35,549.00	$35,549.00	$37,853.00	.25	$2,304.00	$47,316.25
192	1.5.7.2.11	Procure CYSS Material	5 days	Thu 8/9/18	Wed 8/15/18	LBNL	$30,471.00	$30,471.00	$42,918.20	.25	$12,447.20	$53,647.75
193	1.5.7.2.12	Production and test Cylindrical Structural	70 days	Fri 8/10/18	Thu 11/15/18	LBNL	$4,616.00	$4,616.00	$24,776.00	.25	$20,160.00	$30,970.00
194	1.5.7.2.13	Procure COSS Material	5 days	Mon 8/13/18	Fri 8/17/18	LBNL	$50,000.00	$50,000.00	$50,000.00	.25	$0.00	$62,500.00
195	1.5.7.2.14	Procure Shipping and Storage Containers	60 days	Wed 8/1/18	Tue 10/23/18	LBNL	$0.00	$0.00	$0.00	.25	$0.00	$0.00
196	1.5.7.2.15	Procure Detector Half Barrels	100 days	Mon 8/13/18	Fri 12/28/18		$13,000.00	$13,000.00	$14,552.00	.25	$1,552.00	$18,190.00
197	1.5.7.2.16	Procure Service Half Barrels	100 days	Tue 8/14/18	Mon 12/31/18		$120,000.00	$120,000.00	$121,552.00	.25	$1,552.00	$151,940.00
198	1.5.7.2.17	Procure Detector and Service Half Barrels	100 days	Wed 8/15/18	Tue 1/1/19		$21,000.00	$21,000.00	$22,552.00	.25	$1,552.00	$28,190.00
199	1.5.7.2.18	Procure Two Half Support Structures	100 days	Thu 8/16/18	Wed 1/2/19		$51,597.00	$51,597.00	$53,149.00	.25	$1,552.00	$66,436.25
200	**1.5.7.3**	**Assembly and Testing**	**612 days**	**Thu 9/27/18**	**Fri 1/29/21**		**$0.00**	**$14,366.00**	**$312,234.72**		**$297,868.72**	**$384,879.24**
201	1.5.7.3.1	Test Production PB	10 days	Thu 9/27/18	Wed 10/10/18	LBNL	$0.00	$0.00	$11,520.00	.25	$11,520.00	$14,400.00
202	1.5.7.3.2	Ship PB to BNL	5 days	Thu 10/11/18	Wed 10/17/18	LBNL	$0.00	$0.00	$1,152.00	.25	$1,152.00	$1,440.00
203	1.5.7.3.3	Test Power Supplies at BNL	10 days	Fri 10/12/18	Thu 10/25/18	LBNL	$0.00	$0.00	$11,520.00	.25	$11,520.00	$14,400.00
204	1.5.7.3.4	Test Production FEMS, e-Links, CRU, optical	60 days	Mon 4/15/19	Fri 7/5/19	LANL	$0.00	$0.00	$21,600.00	.25	$21,600.00	$27,000.00
205	1.5.7.3.5	Assemble & Test Cooling System	20 days	Mon 12/24/18	Fri 1/18/19	MIT	$0.00	$0.00	$14,400.00	.25	$14,400.00	$18,000.00
206	1.5.7.3.6	Stave Receipt Inspection	10 days	Mon 8/5/19	Fri 8/16/19	LBNL	$0.00	$0.00	$5,760.00	.25	$5,760.00	$7,200.00

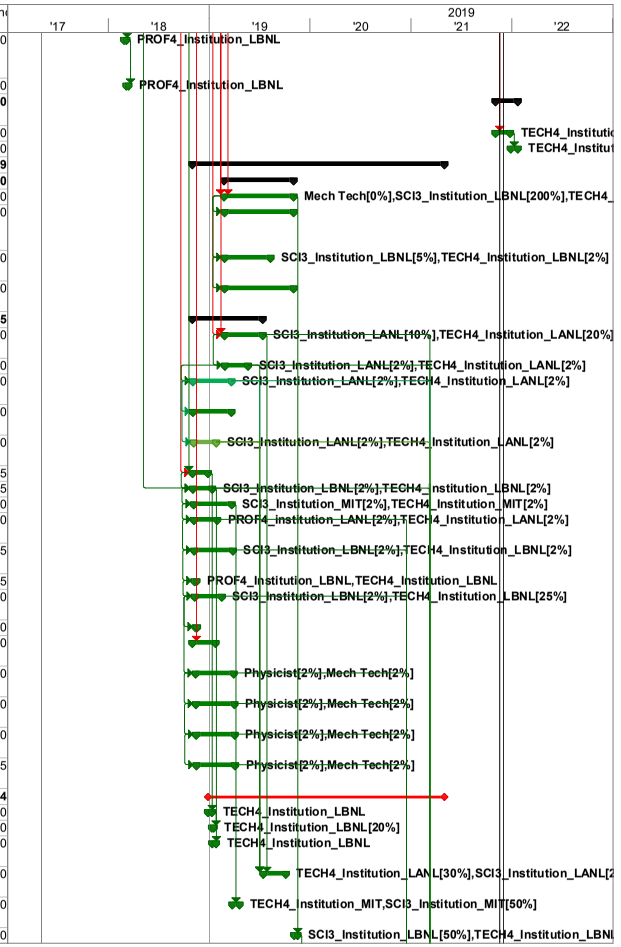

ID	WBS	Task Name	Duration	Start	Finish	Institutic	Fixed Cost	calculate fixed cost	Cost	contingen	Resource Cost	cost+contingen
207	1.5.7.3.7	Individual Stave test and rework	70 days	Mon 8/19/19	Fri 11/22/19	LBNL	$0.00	$0.00	$16,128.00	.25	$16,128.00	$20,160.00
208	**1.5.7.3.8**	**Layer Assembly and Test**	**105 days**	**Mon 11/25/19**	**Fri 4/17/20**	**LBNL**	**$0.00**	**$5,355.00**	**$67,537.64**		**$62,182.64**	**$84,422.05**
209	1.5.7.3.8.1	Test Installation of Staves onto End	20 days	Mon 11/25/19	Fri 12/20/19		$0.00	$0.00	$7,282.88	.25	$7,282.88	$9,103.60
210	1.5.7.3.8.2	Half-Detector Assembly Review	5 days	Mon 12/23/19	Fri 12/27/19	LBNL	$0.00	$0.00	$2,674.88	.25	$2,674.88	$3,343.60
211	1.5.7.3.8.3	Install Staves onto End Wheels	35 days	Mon 12/30/19	Fri 2/14/20	LBNL	$2,770.00	$2,770.00	$24,228.08	.25	$21,458.08	$30,285.10
212	1.5.7.3.8.4	Test and Rework Layers after Assembly	30 days	Mon 2/17/20	Fri 3/27/20	LBNL	$2,585.00	$2,585.00	$16,071.80	.25	$13,486.80	$20,089.75
213	1.5.7.3.8.5	Perform Half Detector Metrology	15 days	Mon 3/30/20	Fri 4/17/20	LBNL	$0.00	$0.00	$17,280.00	.25	$17,280.00	$21,600.00
214	1.5.7.3.8.6	Milestone Complete Layers	0 days	Fri 4/17/20	Fri 4/17/20	LBNL	$0.00	$0.00	$0.00	.25	$0.00	$0.00
215	**1.5.7.3.9**	**Barrel Assembly and Test**	**85 days**	**Mon 4/20/20**	**Fri 8/14/20**	**LBNL**	**$0.00**	**$9,011.00**	**$87,848.44**		**$78,837.44**	**$109,810.55**
216	1.5.7.3.9.1	Assemble Layers and CYSS into Half	40 days	Mon 4/20/20	Fri 6/12/20	LBNL	$0.00	$0.00	$46,372.16	.25	$46,372.16	$57,965.20
217	1.5.7.3.9.2	Test and Rework Half Detector	10 days	Mon 6/15/20	Fri 6/26/20	LBNL	$2,585.00	$2,585.00	$7,934.76	.25	$5,349.76	$9,918.45
218	1.5.7.3.9.3	Perform Half Detector Metrology on Final Assembly	10 days	Mon 6/29/20	Fri 7/10/20	LBNL	$0.00	$0.00	$11,520.00	.25	$11,520.00	$14,400.00
219	1.5.7.3.9.4	Validation of Final Assembly	15 days	Mon 7/13/20	Fri 7/31/20	LBNL	$2,585.00	$2,585.00	$13,201.64	.25	$10,616.64	$16,502.05
220	1.5.7.3.9.5	Pack/ship Final Assemblies to BNL	10 days	Mon 8/3/20	Fri 8/14/20	LBNL	$3,841.00	$3,841.00	$8,819.88	.25	$4,978.88	$11,024.85
221	1.5.7.3.10	Metrology on Stave Assemblies	30 days	Mon 8/17/20	Fri 9/25/20	LBNL	$0.00	$0.00	$17,880.00	.25	$17,880.00	$22,350.00
222	1.5.7.3.11	Assemble full Ladders into Half support	50 days	Mon 9/28/20	Fri 12/4/20	LBNL	$0.00	$0.00	$24,832.00	.25	$24,832.00	$31,040.00
223	1.5.7.3.12	Metrology on Final Assembly	10 days	Mon 12/7/20	Fri 12/18/20	LBNL	$0.00	$0.00	$10,400.00	.25	$10,400.00	$13,000.00
224	1.5.7.3.13	Half detector Assembly Readout and Cooling	30 days	Mon 12/21/20	Fri 1/29/21		$0.00	$0.00	$21,656.64	0	$21,656.64	$21,656.64
225	**1.5.8**	**Installation**	**131 days**	**Mon 2/1/21**	**Mon 8/2/21**		**$0.00**	**$0.00**	**$45,248.00**		**$45,248.00**	**$63,160.00**
226	1.5.8.1	Installation Prep	10 days	Mon 2/1/21	Fri 2/12/21	ALL	$0.00	$0.00	$15,520.00	.25	$15,520.00	$19,400.00
227	1.5.8.2	Installation Review	1 day	Mon 2/15/21	Mon 2/15/21	ALL	$0.00	$0.00	$2,080.00	.10	$2,080.00	$2,288.00
228	1.5.8.3	Installation	30 days	Tue 2/16/21	Mon 3/29/21	ALL	$0.00	$0.00	$27,648.00	.50	$27,648.00	$41,472.00
229	1.5.8.4	Commissioning	90 days	Tue 3/30/21	Mon 8/2/21		$0.00	$0.00	$0.00	0	$0.00	$0.00
230	1.5.9	Ready for beam	0 days	Mon 8/2/21	Mon 8/2/21		$0.00	$0.00	$0.00	0	$0.00	$0.00

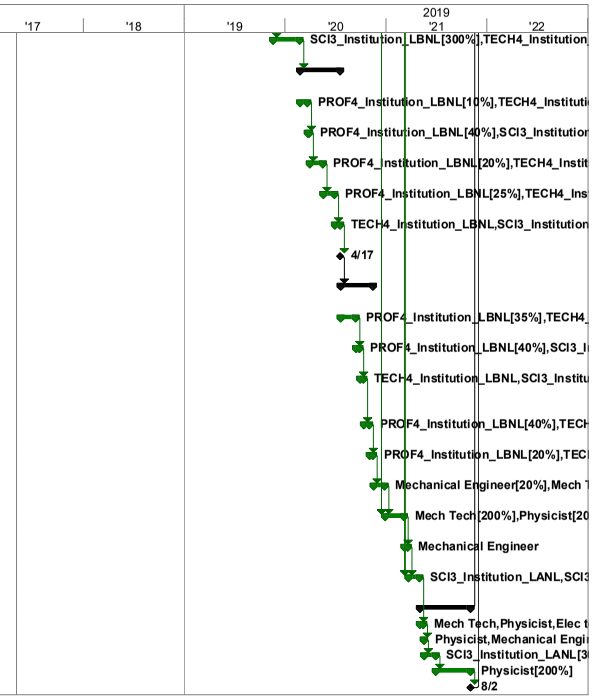

Here we attached the full project file

10 Abbreviations and Code Names

MAPS	Monolithic Active Pixel Sensors
MVTX	MAPS-based Vertex Detector
QGP	Quark Gluon Plasma
DCA	Distance of Closest Approach
RHIC	Relativistic Heavy Ion Collider at BNL
LHC	Large Hadron Collider at CERN

11 Literature Cited

References

[1] A. Adare et al. Energy Loss and Flow of Heavy Quarks in Au+Au Collisions at $\sqrt{s_{NN}}$ = 200 GeV. *Phys. Rev. Lett.*, 98:172301, 2007.

[2] B.I. Abelev et al. Transverse Momentum and Centrality Dependence of High-p_T Nonphotonic Electron Suppression in Au+Au Collisions at $\sqrt{s_{NN}}$ = 200 GeV. *Phys. Rev. Lett.*, 98:192301, 2007.

[3] L. Adamczyk et al. Observation of D^0 Meson Nuclear Modifications in Au+Au Collisions at $\sqrt{s_{NN}}$ = 200 GeV. *Phys. Rev. Lett.*, 113(14):142301, 2014.

[4] Betty Abelev et al. Suppression of high transverse momentum D mesons in central Pb-Pb collisions at $\sqrt{s_{NN}}$ = 2.76 TeV. *JHEP*, 09:112, 2012.

[5] J.C. Xu, J.F. Liao, and M. Gyulassy. Bridging soft-hard transport properties of quark-gluon plasmas with cujet3.0. *JHEP*, 1602:169, 2016.

[6] L. Adamczyk et al. Measurement of D^0 azimuthal anisotropy at mid-rapidity in Au+Au collisions at $\sqrt{s_{NN}} = 200$ GeV. 2017.

[7] S.K. Das, F. Scardina, S. Plumari, and V. Greco. Heavy-flavor in-medium momentum evolution: Langevin versus boltzmann approach. *Phys. Rev.*, C90:044901, 2014.

[8] Serguei Chatrchyan et al. Evidence of b-Jet Quenching in PbPb Collisions at $\sqrt{s_{NN}} = 2.76$TeV. *Phys. Rev. Lett.*, 113(13):132301, 2014. [Erratum: Phys. Rev. Lett.115,no.2,029903(2015)].

[9] Jinrui Huang, Zhong-Bo Kang, and Ivan Vitev. Inclusive b-jet production in heavy ion collisions at the LHC. *Phys. Lett.*, B726:251–256, 2013.

[10] sPHENIX preConceptual Design Report. 2015.

[11] A. Adare et al. An Upgrade Proposal from the PHENIX Collaboration. 2015.

[12] B Abelev et al. Technical Design Report for the Upgrade of the ALICE Inner Tracking System. *J. Phys.*, G41:087002, 2014.

[13] Gianluca Aglieri Rinella. The ALPIDE pixel sensor chip for the upgrade of the ALICE Inner Tracking System. *Nucl. Instrum. Methods Phys. Res., A*, xx:xx, 2016. In Press.

[14] M. Mager. ALPIDE, the Monolithic Active Pixel Sensor for the ALICE ITS upgrade. *Nucl. Instrum. Meth.*, A824:434–438, 2016.

[15] CMS Collaboration. Transverse momentum balance of b-jet pairs in PbPb collisions at 5 TeV. 2016.

[16] E. Norrbin and T. Sjostrand. Production and hadronization of heavy quarks. *Eur. Phys. J.*, C17:137–161, 2000.

[17] Jinrui Huang, Zhong-Bo Kang, Ivan Vitev, and Hongxi Xing. Photon-tagged and B-meson-tagged b-jet production at the LHC. *Phys. Lett.*, B750:287–293, 2015.

[18] CMS Collaboration. Splitting function in pp and PbPb collisions at 5.02 TeV. 2016.

[19] K Kauder. Measurement of the Shared Momentum Fraction zg using Jet Reconstruction in p+p and Au+Au Collisions with STAR. 2016.

[20] Andrew J. Larkoski, Simone Marzani, Gregory Soyez, and Jesse Thaler. Soft Drop. *JHEP*, 05:146, 2014.

[21] S. S. Cao, G.Y. Qin, and S. A. Bass. Energy loss, hadronization and hadronic interactions of heavy flavors in relativistic heavy-ion collisions. *Phys. Rev.*, C92:024907, 2015.

[22] Min He, Rainer J. Fries, and Ralf Rapp. Heavy-Quark Diffusion and Hadronization in Quark-Gluon Plasma. *Phys. Rev.*, C86:014903, 2012.

[23] J. Anderson et al. FELIX: a PCIe based high-throughput approach for interfacing front-end and trigger electronics in the ATLAS Upgrade framework. *JINST*, 11(12):C12023, 2016.

[24] S. Adler et al. Phenix on-line systems. *Nucl. Instrum. Meth. A*, 499:560, 2003.

[25] S. Agostinelli et al. GEANT4: A Simulation toolkit. *Nucl. Instrum. Meth.*, A506:250–303, 2003.

[26] Johannes Rauch and Tobias Schlter. GENFIT a Generic Track-Fitting Toolkit. *J. Phys. Conf. Ser.*, 608(1):012042, 2015.

[27] Wolfgang Waltenberger. RAVE: A detector-independent toolkit to reconstruct vertices. *IEEE Trans. Nucl. Sci.*, 58:434–444, 2011.